Universiteit Utrecht

if technology

The Patuha geothermal system: a numerical model of a vapor-dominated system

By Martijn Schotanus 3183335

Version 2, April 2013

MSc Thesis supervisors

Prof. Dr. Ruud J. Schotting - UU

N. A. Buik MSc. BBE. - IF Technology

Dr. M. Gutierrez-Neri - IF Technology/EBN

Abstract

The Patuha geothermal system is a vapor-dominated reservoir located about 40 kilometers southwest of Bandung on western Java, Indonesia. The geothermal system consists of a cap rock, an underlying steam cap and a deep liquid-dominated reservoir. The reservoir is provided with heat by a main heat source below Kawah Putih and the Patuha volcano. The flow of fluid takes place through fault zones and in the low permeability reservoir rock.

A straightforward numerical model of the system has been developed in Petrasim, which is a graphical interface of TOUGH2. The modeled reservoir consists of three homogeneous segments: the cap rock and (vapor- and liquid-dominated) reservoir rock, which are crosscut by fault zones initiating vertical fluid flow. It has been demonstrated in this study that the Patuha vapor-dominated reservoir resembles the theoretical design for a vapor-dominated geothermal system. The Patuha geothermal system can thus be represented by such a simple and straightforward model.

Contents

List of Figures

List of Tables

1 Introduction

Indonesia has the largest potential resources of geothermal energy worldwide. The total potential for Indonesia is estimated at 27,000 MW (Dharma, 2010). Its current installed capacity is about 1,200 MW, which is approximately 4% of the total energy supply. Since this is only a fraction of the total potential for geothermal energy, the Indonesian government introduced policy which should help increase the total capacity by at least 50% in the coming years (Bertani, 2010).

Since the development of new geothermal resources requires large investments and will take several years, the main focus is on increasing the production rate of existing power plants. One of the Indonesian geothermal resources with high potential is the Patuha vapor-dominated resource. There are already several wells drilled in the area, but the production of geothermal heat has not been started yet. Therefore, the Patuha resource is of great interest for Indonesia in order to increase the total geothermal capacity on a short term. Extensive research has already been carried out in the area. The available data is reviewed in this thesis and is used to develop a numerical model of the reservoir.

The structure of this thesis is based on a step-wise development plan of a geothermal system in a volcanically active environment. Preliminary research starts by mapping the sources of data which are accessible at the surface: geological setting, surface geology (Chapter 3) and surface manifestations (Chapter 4). Both include information on the (volcanic) activity of the area. The type and distribution of the surface manifestations can even be used to give an indication of subsurface properties, such as location of up and outflow zones and presence of high permeability zones.

Then an analysis of the chemistry of the surface manifestation waters is conducted (Chapter 4). This data holds valuable information on the flow path origin of the geothermal fluids and on the interaction between the fluids and the surrounding rock.

Mapping at the subsurface has been carried out using electrical resistivity and gravimetric methods (Chapter 5). These can be used to interpret the subsurface geology and locate the fault zones in the area. Combined with the location of the surface manifestations this gives a good approximation of the subsurface structures. There are other methods to obtain useful data, like remote sensing and seismic survey, but these were not applied during the development of the Patuha geothermal resource.

Since there are already several wells present in the area, an analysis of the data obtained from these wells has been carried out. The well geology shows the exact depth of important features, such as the presence of altered minerals. Measurements from the wells also give the temperature and pressure distribution of the reservoir. Therefore important subsurface properties of the system can be quantified (Chapter 7).

Using a combination of theoretical and field data, a simple conceptual model of the system can be developed (Chapter 8). This will be implemented in a three-dimensional reservoir model (Chapter 9). The numerical model is used to compare the optimal theoretical pressure and temperature conditions of a vapor-dominated geothermal system to the data obtained from the wells.

2 Geothermal energy in Indonesia

2.1 Introduction

Indonesia has the highest geothermal potential in the world. The size of the resources is estimated to be over 27,000 MW, which is approximately forty percent of the world's total geothermal energy potential (Darma et al., 2010, Dwipa et al., 2005). With an installed capacity of only about 1,200 MW in 2010 (Bertani, 2010), the archipelago of Indonesia is staying behind compared with countries like the Philippines and the United States. Although the resources of these countries are much less, the installed capacity surpasses that of Indonesia with respectively 1,904 MW and 3,093 MW (Bertani, 2010).

In an attempt to reduce the dependence on fossil fuels as a single source of energy production, the Indonesian government has introduced policy to attract investors in geothermal energy (Darma et al., 2010). This should lead to an increase of the installed capacity by 50% (approximately 3,500 MW) in 2015 (Bertani, 2010).

The geothermal resources of Indonesia are mainly concentrated on the islands of Sumatra, Java-Bali and Sulawesi (Table 1). Since 1982, several geothermal prospects were realized on these islands: Kamojang (200 MW), Salak (377 MW), Darajat (260 MW), Wayang Windu (227 MW), Dieng (60 MW) on Java, Sibayak (13.3 MW) in North Sumatera and Lahendong (60 MW) in North Sulawesi (Darma et al., 2010). Because the island of Java is the most populous islands in the world, the electricity demand on this island is the largest of the Indonesian archipelago. Correspondingly, the power grid on Java is the most advanced of Indonesia. Therefore the installed capacity is the largest on Java.

Table 1 Indonesia's geothermal potential (Dwipa et al., 2005)

Location	**Resources (MWe)**		**Reserves (MWe)**		
	Speculative	Hypothetical	Possible	Probable	Proven
Sumatra	5705	2433	5419	15	499
Java-Bali	2300	1611	3088	603	1727
Nusa Tenggara	150	438	631	-	14
Sulawesi	1000	125	632	110	65
Maluku/Irian	325	117	142	-	-
Kalimantan	50	-	-	-	-
Total (251 locations)	**9530**	**4714**	**9912**	**728**	**2305**
	14244		12945		
			27189		

2.2 Geothermal systems on Java

In 1978, the first geothermal power plant in Indonesia was commissioned in Kamojang, West Java. Since then, almost 1,200 MW of installed capacity was established. Of this capacity, about 94% is installed on the island of Java. The most important geothermal systems will be discussed in the following paragraph.

Kamojang

The first exploited geothermal field in Kamojang, located 40 km southeast of Bandung, produced only 250 kW. Now the installed capacity of the Kamojang field is 200 MW, and an additional 60 MW is under construction. Kamojang is a vapor-dominated system with an average temperature and pressure 245°C and 35 bars (Fauzi et al., 2000).

Salak

Gungung Salak is located 70 km south of Jakarta. The geothermal field produces 377 MW, divided over six different power plants. The production started in 1994 with the installation of two units and in 1997 the production was increased to its present capacity. The Salak field is a liquid-dominated reservoir with initial temperatures ranging between 235°C and 310°C (Acuna et al., 2008)

Darajat

Darajat is a vapor-dominated system with a temperature of approximately 245 °C, which is operative since 1994. The initial production was 110 MW, which was increased to 270 MW with the installation of a second unit in 2008 and an upgrade of the older unit. It is located a few kilometers south of the Kamojang field (Darma et al., 2010).

Wayang Windu

The Wayang Windu field is located a few kilometers west of the Kamojang and Darajat geothermal fields (about 40 km south of Bandung). The field is in operation since 2000, producing 110 MW, and upgraded in 2009 with an additional 117 MW. The reservoir is liquid-dominated with temperatures ranging from 250°C to 270°C (Fauzi et al., 2000).

Dieng

While the systems mentioned earlier are all located West Java, Dieng is the only producing field in Central Java. The field is located 60 km southwest of Semarang. Although a 60 MW unit was installed in 1998, it only started producing in 2002. The geothermal system is dominated by two-phase conditions and high temperatures of 280°C to 330°C (Fauzi et al., 2000).

The different geothermal systems mentioned above are all producing electricity and thereby adding to the installed capacity of geothermal in Indonesia. There are also several geothermal fields on Java which are in an advanced stage of development, for example the Patuha and Karaha-Telaga Bodas fields.
Both systems are located on West Java. Patuha lies about 40 km southwest of Bandung, about 15 km west of the Wayang Windu field. The Karaha-Telaga Bodas field is located about 30 km west of the Darajat geothermal system, near the Galunggung volcano.
The liquid-dominated system of Karaha-Telaga Bodas is overlain by a steam cap and shows temperatures of 250°C up to 353°C (Nemčok et al., 2007). The steam reservoir temperatures of the Patuha field range from 209°C to 241°C (Layman et al., 2003). Both fields are expected to start their production in the next couple of years.

2.3 Type of geothermal systems

Table 2 shows a simple classification of geothermal systems based on several reservoir properties, such as reservoir equilibrium state, fluid type, temperature and elevation differences (Nicholson, 1993). The geothermal systems mentioned in the previous Paragraph are all volcanogenic, with magma providing the driving heat flux. These systems can all be classified as high temperature dynamic systems in areas with steep topography and can further be subdivided into liquid- or vapor-dominated systems, based on the fluid type.

Table 2 A classification of geothermal systems (Nicholson, 1993)

A classification of geothermal systems	
Dynamic systems (convective)	***Static systems (conductive)***
High temperature	**Low-temperature**
Liquid-dominated	**Geopressurised**
Low-relief	
High-relief	
Vapor-dominated	
Low-temperature	

Most geothermal systems are liquid-dominated. These reservoirs contain water in all the channelways and interstitial pores (Sigurdsson et al., 1999). The pressure and temperature will increase naturally with depth (Figure 1a). The maximum temperatures within these reservoirs are approximately 370°C.
In areas marked by high relief, like the island-arc system in Southern Indonesia, the steep topography prevents chloride fluids to reach the surface at the highest elevations. These fluids flow laterally to areas of lower topography, where they discharge. Along this flowpath, the chloride fluids can be diluted with groundwater or they can mix with descending sulphate waters and steam condensates. The acid sulphate

waters and steam condensates originate in a two-phase zone at several hundred meters deep. These waters are also discharged directly near the upflow zone as fumaroles, steaming ground and acidic sulphate-water hot springs (Nicholson, 1993).

Surface manifestations, like fumaroles, steaming ground and acidic sulphate-water hot springs, are also very common for vapor-dominated systems in the near surroundings of the upflow zone, since steam is the main fluid component in the reservoir. As the steam rises it can discharge through fractures and originate in these surface manifestations, or they can flow laterally along the base of a sealing low-permeability layer. The steam cools down and condenses. It can either descend into the deep reservoir for recirculation or discharge as hot springs at lower elevations. The composition of these discharge waters can vary along the flow path, since the less soluble gases remain in the gas phase and the fluid chemistry is also changed by contact with the surrounding rock and/or other fluids.

The pressure and temperature distribution in vapor-dominated systems is different from that of liquid-dominated systems. Within the reservoir, the pressure and temperature are constant near the maximum enthalpy of "dry" steam, which is about 240°C and 3.3 MPa. This steam in the reservoir is present in the open cracks, fractures and faults. The intergranular pore space is filled with liquid (Figure 1b) (Sigurdsson et al., 1999). The Patuha geothermal system is considered to be vapor-dominated, therefore these types of systems are explained further in the next paragraph.

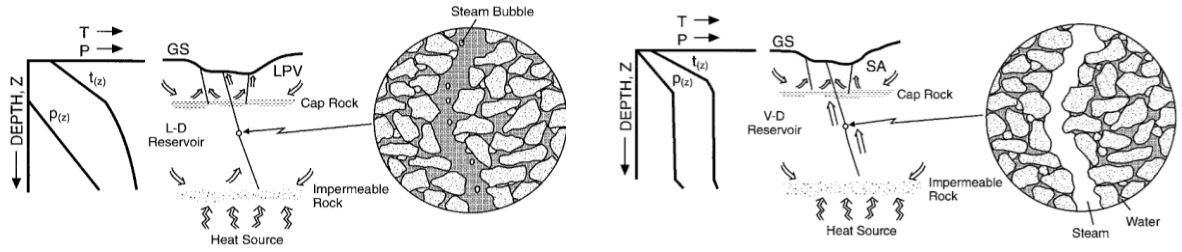

Figure 1 Schematic model of a liquid-dominated system (a) and a vapor-dominated system (b) (Sigurdsson et al., 1999)

2.4 Vapor-dominated systems

The natural occurrence of vapor-dominated systems is very rare. Besides from the Patuha system, only four systems are described in the literature as vapor-dominated reservoirs which extend over large ranges in depth: The Geysers (California, US), Lardarello (Italy), Kamojang and Darajat (Java, Indonesia). Apart from these large vapor-dominated systems, there are many hydrothermal reservoirs with small vapor-dominated zones which are very localized, confined to a few fractures or fracture zones (Ingebritsen and Sorey, 1988). There are three general models for hydrothermal convection systems that include vapor-dominated zones, as proposed by Ingebritsen and Sorey (1988) (Figure 2). The following paragraph gives a description of these three conceptual models proposed by these authors.

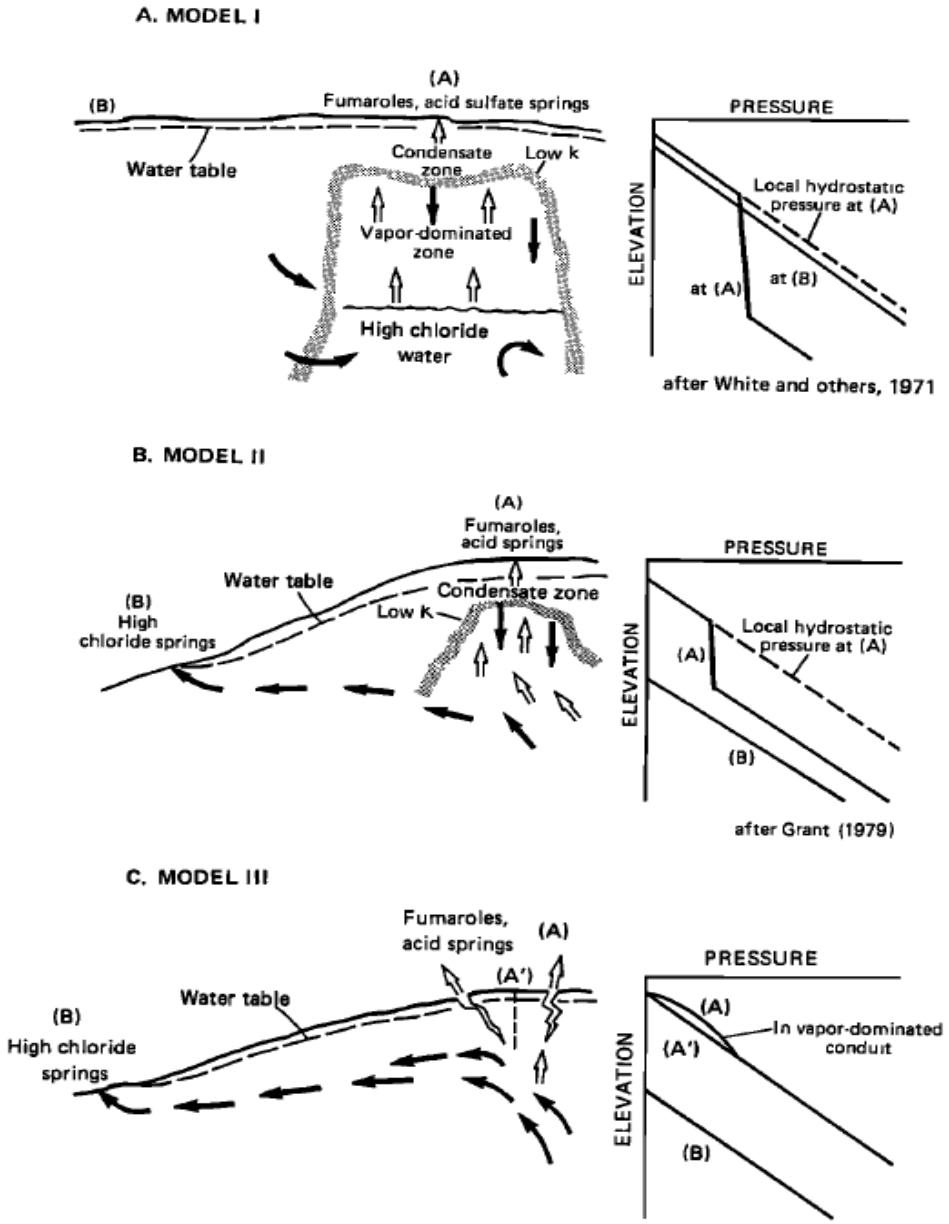

Figure 2 Conceptual models of three hydrothermal convection systems that include vapor-dominated zones. Solid arrows are for liquid, and open arrows are for steam (Ingebritsen and Sorey, 1988).

Model I represents an extensive vapor-dominated zone. As shown in Figure 2 (a), the zone is generally underpressured with respect to the local hydrostatic pressure. Such a system can only exist, when it is isolated from the surrounding flow systems by a low-permeability barrier, usually referred to as cap rock. Initially, all vapor-dominated systems were probably liquid dominated. Evidence for this is found in the presence of minerals (Paragraph 3.2.3) which are indicative for liquid-dominated conditions (Allis, 2000). The formation of the low permeability barrier can be due to the deposition of silica as a result of cooling of reservoir fluids in the shallower parts of the system or by the deposition of calcite, gypsum or anhydrite due to the heating (and vaporization) of recharge waters. However, the presence of this barrier can also be related to the process of argillization, where certain minerals are converted into clay minerals due to

hydrothermal alteration, or to the geological structure and lithologic contrast (Ingebritsen and Sorey, 1988). It is assumed that the recharge of the system takes place from the base of the reservoir, because the recharge from the sides and top of the flow system is limited by the presence of the low-permeability barrier. Also, it is assumed that these vapor-dominated zones are overlaying a zone of high-temperature liquid, although there is no direct evidence for liquid throughflow from below. In addition, a very intense local (magmatic) heat source is required, since a vapor-dominated system requires an intense heat input at the base and the throughflow of fluids is limited.

The heat transport within the vapor-dominated systems is controlled by the rising steam. At the top of these zones, the heat is released, what results in a condensate zone. The presence of faults and fractures in the cap rock causes the upward flow of fluids. This results in the formation of fumaroles (openings in the Earth's crust) and other, highly acidic, surface manifestations which are indications for the presence of vapor-dominated zones. In this model, the density difference is the controlling factor for fluid circulation. Therefore, the flow direction is mainly vertical.

In models II and III (Figure 2 (b) and (c)), the vapor-dominated zones are much smaller and the throughflow of liquid is more important. The driving force of the fluid flow in these two models is the elevation difference between the steam heated features and the (high-chloride) hot springs.

In model II, this elevation between the fumaroles and hot springs as well as the pressure gradient required to drive the lateral flow controls the maximum thickness of the vapor-dominated zone. Large topographic relief is therefore of great importance in the formation and evolution of model II-type vapor-dominated zones. The lateral outflow is initiated by a change in hydrologic or geologic conditions after a period of convective heating in an upflow zone. The vapor-dominated zone in model II also needs a low-permeability barrier in order to inhibit the movement of cold water into the evolving vapor-dominated zone.

Model III-type vapor-dominated zones are relatively simple. These zones are restricted to faults or fractures with a high vertical permeability. No changes in rock properties or boundary conditions are necessary for the formation of such Model III-type systems. It only needs the circumstances that allow a high rate of steam upflow from an area of phase separation. In contrast with Model I and II, the pressure profile of Model III does not show a fast pressure drop and the pressure is never below hydrostatic. The conditions of this system are not sufficient to evolve to a Model II-type system, since there is no low-permeability zone to act as a sealing layer.

The largest two vapor-dominated systems, The Geysers and Lardarello, are best described as Model I-type system. However, most natural systems are too complex to comprehend in one simple model. Therefore naturally occurring vapor-dominated geothermal systems can better be represented as a combination of these models (Ingebritsen and Sorey, 1988). The Indonesian systems (Kamojang and Darajat) show similar properties as described for Model I, but their reservoirs are relatively small and the large variations in topography play an important role in the flow patterns of these systems. Therefore the Indonesian systems are probably best described as a combination between Model I and II.

2.5 Evolution of vapor-dominated systems and their system properties

As mentioned before, vapor-dominated systems evolved from systems that were initially hot-water systems. This process can be initiated by an increasing heat input to the system or by a decreasing permeability as a result of self-sealing. In these cases, it becomes possible that water lost by discharge can no longer be entirely replaced by recharge. This results in an underpressured reservoir and a vapor-dominated system starts to evolve (White et al., 1971).

It is generally assumed that the evolution and therefore the properties of such large vapor-dominated systems can differ from each other mainly based on the geological setting. The systems in The Geysers and Lardarello are surrounded by naturally low permeability rock, thereby limiting the inflow of meteoric waters. The low pressures in these systems are thought to be caused and/or sustained by factors such as reservoir dilation and steam loss to the surface. Both The Geysers and Lardarello have large reservoir areas (~100 km2), low heat flow intensities and long lifespans (>10^5 years) (Allis, 2000).

The Kamojang and Darajat systems are both volcano-hosted, meaning they probably consist of a vapor chimney above the main magmatic plume which is surrounded by a liquid-dominated geothermal system. The vapor chimney can decay into an under-pressured vapor-dominated system due to magmatic-hydrothermal activity and increasingly lower permeability of the host volcano. These systems are restricted to volcanic arcs where the subduction is perpendicular to the trench/for-arc region. The heat flow intensity of Darajat and Kamojang is an order of magnitude larger than The Geysers and Lardarello, implying that the infiltration rate of meteoric waters is much larger and the lifespan of the vapor system is shorter (< 10^4) (Allis, 2000).

2.6 The Patuha geothermal system

From pressure and temperature measurements at depth, it can be concluded that the Patuha geothermal system is vapor-dominated, as will be discussed in Paragraph 7.4. The Patuha geothermal system is situated in a similar geological setting as the Darajat and Kamojang systems. The evolution and general properties of geothermal systems are mainly controlled by the geological setting, as stated in Paragraph 2.5. Therefore, it can be assumed that the Patuha system will have similar properties as the geothermal systems in Darajat and Kamojang. Based on these general assumptions, the Patuha system can also be categorized as combination of a Model I- and Model II-type vapor-dominated system.

3 Geology of the Patuha geothermal system

3.1 Tectonic setting of the Java region

The tectonics of the Indonesian region are dominated by the convergence of three large plates: the Eurasian, the Pacific and the Indo-Australian plate. The Pacific and Indo-Australian are moving respectively west-northwest and north relatively to the Eurasian plate. This subduction process is marked by the formation of the Sunda and Java Trench (Figure 3). On the west side of Sumatra the volcanic belt has a southeast orientation, corresponding with the southeast orientation of the Sunda trench. The Java trench, following the Sunda trench, runs from west to east. The downward process of these plates is recorded by seismically active zones, which dip as deeply as 700 km into the mantle (Hamilton, 1979). Formation of volcanoes on Java occurs primarily above the parts of the seismic zone between 100 and 200 km deep. This results in the formation of a volcanic belt, which clearly follows the convergent plate boundary (Figure 4).

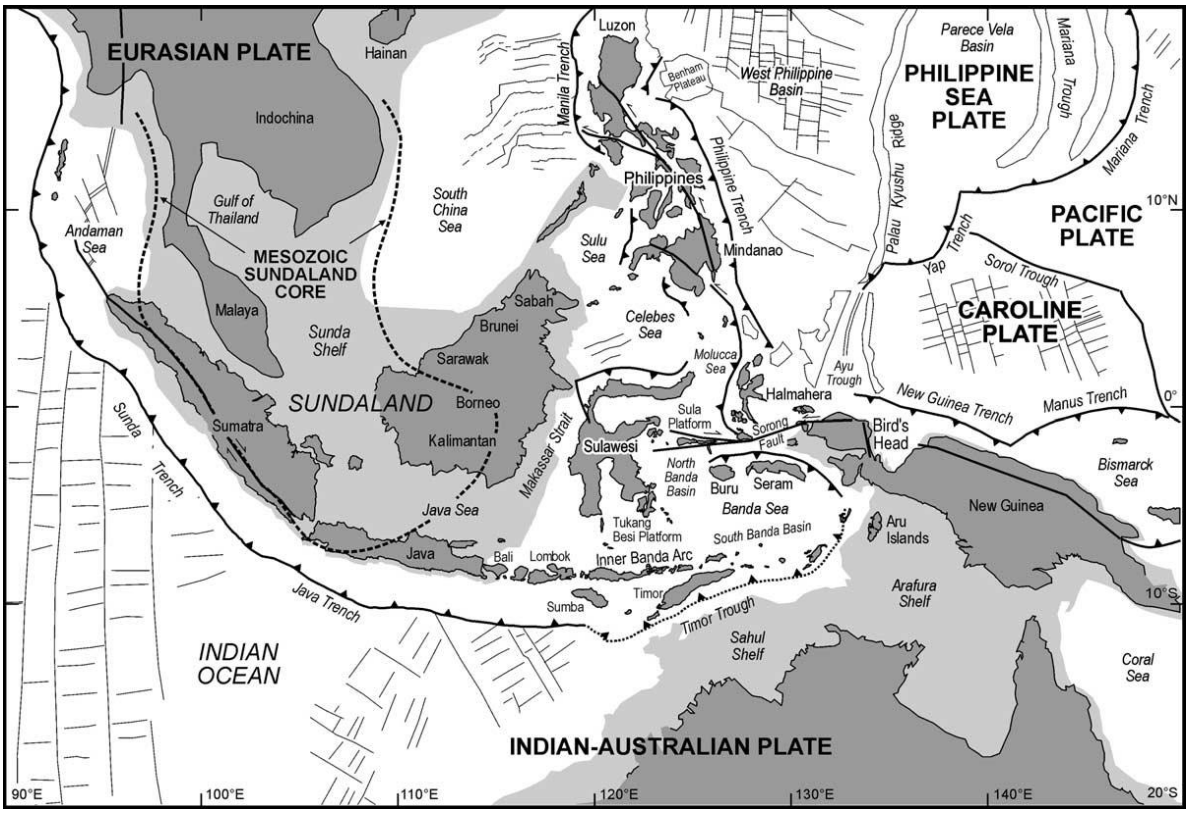

Figure 3 Complex tectonic situation of the Indonesian region (Hall, 2002)

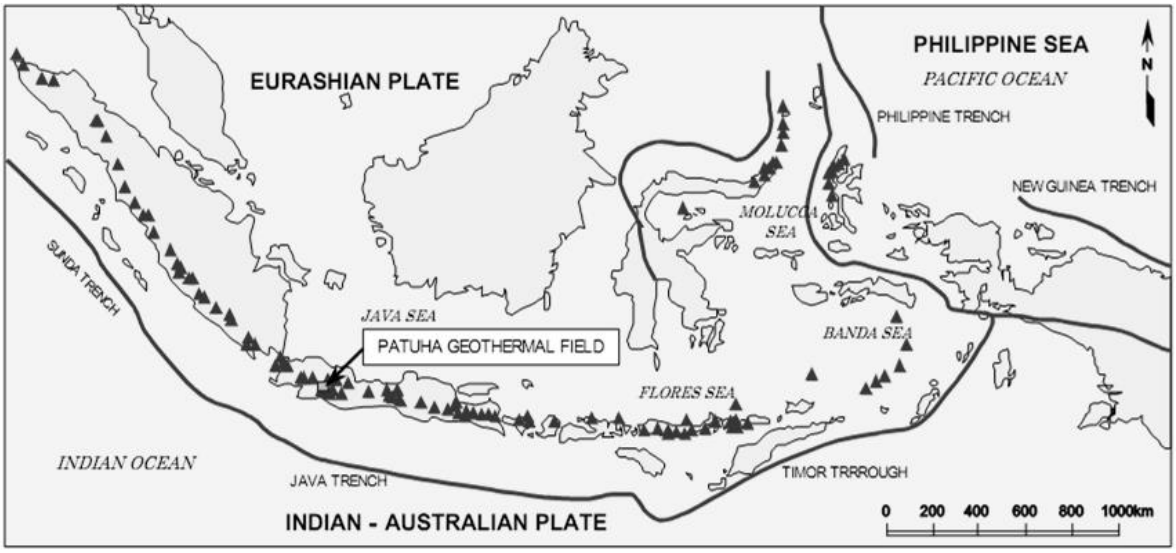

Figure 4 Tectonic map of the Indonesian Archipelago (West JEC, 2007)

3.2 Geological setting of the Patuha geothermal system

3.2.1 Location

The Patuha geothermal system is situated on the island of Java in the West Java Province, approximately 30 kilometers southwest of Bandung (capital city of West Java Province). The concession area spreads on the Bandung District and Cianjur District and is approximately 350 km2 (18 km from north to south and 20 km from east to west). Within the Patuha field, there is the Yala TEKNOSA concession area. This field is situated near the Cibuni crater and is approximately 10 km2 (3.7 km for north to south and 2.6 km from east to west).

The area is marked by several mountains with peaks over 2000 m above sea level with an overall northwest to southeast alignment. Among these peaks are Mt. Kendeng, Mt. Masigit, Mt. Patuha, Mt. Urug and Mt. Waringin.

3.2.2 Volcanism

As mentioned before, in the surroundings of the Patuha field, the mountains are arranged from west-northwest to east-southeast. On a smaller scale there is a different trend in alignment. Volcanoes arrange north-northwest to south-southeast. Such local alignments opposite to the general trend are often identified in island arc systems. The local stress field resulting from the tectonic field around the plate boundary is often mentioned as an explanation for this phenomenon (West JEC, 2007).

The main volcano in the Patuha field is Mt. Patuha. Mt. Patuha is an andesitic stratovolcano (Layman et al, 2003). There are two volcanic craters on the mountain, which lie about 600 m apart: the northwestern crater, near the highest point of the mountain, and the southeast crater. The southeast crater is filled with water, forming a crater lake known as Kawah Putih.

The Patuha field is dominantly covered by volcanic depositions (Figure 5). These depositions are determined to be andesitic lavas and pyroclastics coming from Mt. Patuha and Mt. Kendeng. There is no

record of any historic eruptions (Sriwana et al., 2001), but the depositional rocks are dated as late Pliocene to Quaternary (Layman et al, 2003). Although the latest volcanic eruption in the area is at least 0.12 million years ago (Layman et al, 2003), there are still numerous hydrothermal surface features which are indicative for active volcanism.

3.2.3 Surface geology

The regional geology is dominated by Quaternary volcanic rocks, which cover most of the Patuha field, and Tertiary sedimentary rocks. A map of the regional geology is given in Figure 5. South of the concession area, Tertiary sedimentary outcrops have been identified, while north and west of the Patuha field Tertiary volcanic rocks are dominant. Figure 6 shows the surface geology in the main area of the Patuha field. Table 3 gives a description of the formations which were found in the area.

In the Patuha field, no structural faults were identified at the surface, due to deposition of relatively young volcanic rocks. In the surrounding area, the faults are mainly trending northwest to southeast and east-northeast to west-southwest (Figure 5), corresponding to the regional tectonics.

Table 3 Geological formations found in the Patuha region (West JEC, 2007)

Volcanic formation	Location of outcrop	Age	Description/composition
Undivided pyroclastics	Western and northern side of the Patuha field	Pliocene and Pleistocene	Andesitic breccia, tuff breccia and lapilli tuff
Mt. Kendang	Covering the Patuha field (and thereby the undivided pyroclastics)	Quaternary	Lahar and lava
Mt. Patuha	Covering the Patuha field (and thereby the undivided pyroclastics)	Quaternary	Lahar and lava

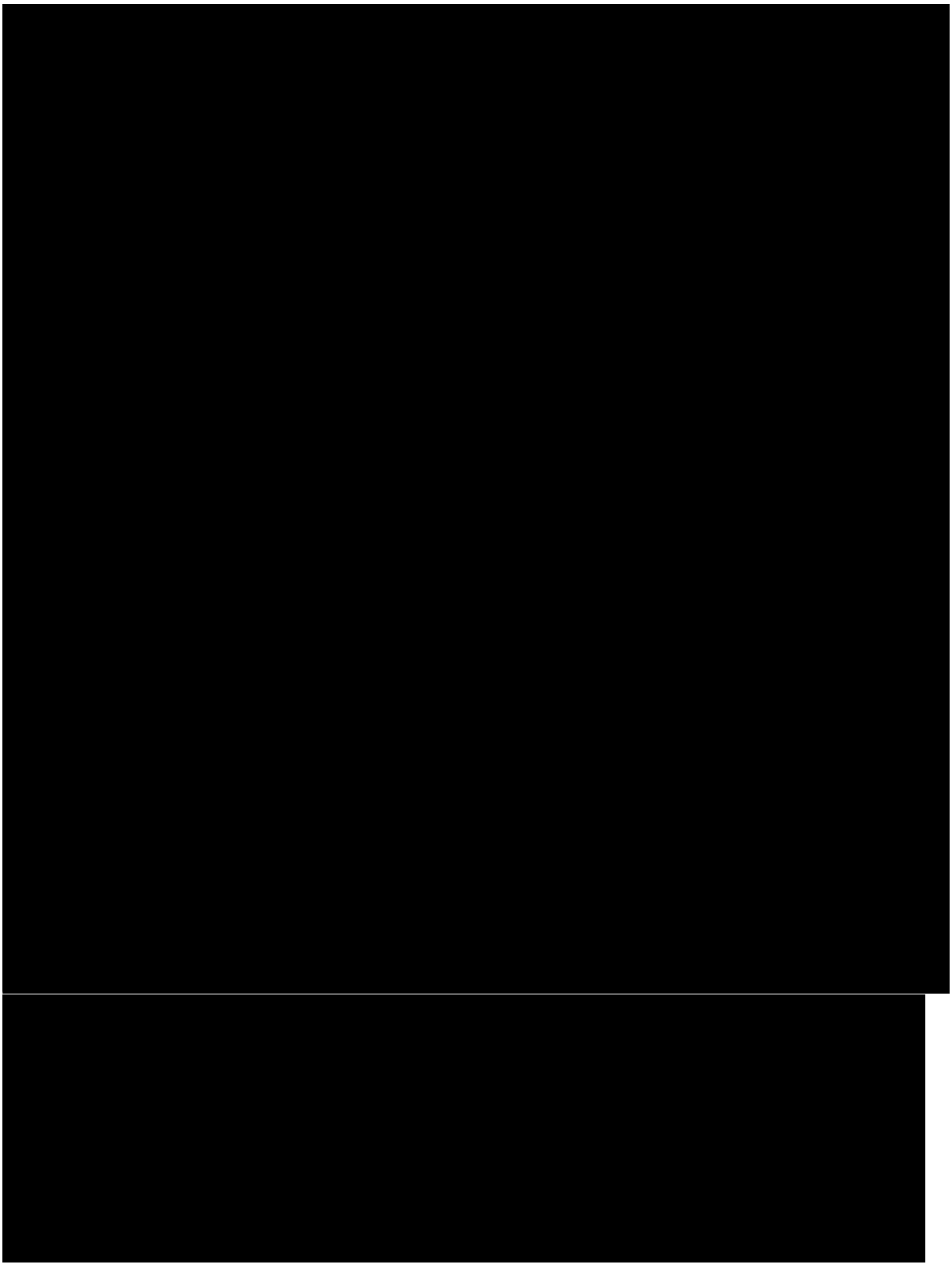

Figure 5 Geologic map of the region of the Patuha field (West JEC, 2007)

Figure 6 Geological map of the main area of the Patuha Geothermal Field (West JEC, 2007)

3.3 Hydrothermal alteration

Hydrothermal alteration is very common in areas of geothermal activity. This mineralogical alteration process is initiated by the contact between hydrothermal fluids and the reservoir rock. At the surface, these altered minerals occur in vicinity of geothermal manifestations. Alteration in the subsurface occurs mainly in zones of high permeability, since in these zones de flow of fluid is best supported.

There are several types of hydrothermal alteration, of which propylitic and argillic alteration are the most important in vapor-dominated geothermal systems. These types of alteration lead to a wide range of hydrothermal minerals that can be recognized in these systems. In general it can be stated that the formation of hydrothermal minerals is affected by several factors, such as temperature, pressure, rock type, permeability, fluid composition and duration of activity (Browne, 1978). Propylitization is a type of alteration which mainly occurs at high temperatures, ranging between 160°C and 351 °C. This type of hydrothermal alteration results in minerals like epidote, chloride and albite (Norman et al., 1991). Argillic

alteration occurs typically at lower temperatures and results in the formation of clay minerals, such as kaolinite, smectite and smectite-illite.

The presence of specific minerals at a certain depth can be a good indicator for the temperature distribution, since many of these minerals can only be formed within a specific range of temperature conditions (Figure 7). Since temperatures in vapor-dominated systems typically do not exceed 240°C (temperature of max. enthalpy of steam), secondary minerals that are generally formed at higher temperature conditions are an indication for liquid-dominated conditions in an earlier stage. An example of such an alteration mineral is epidote. Epidote is very common in active geothermal systems and is an indicator for high temperatures (usually above 240-260°C). However, epidote is also encountered in vapor-dominated reservoirs. It is suggested that in these cases, the epidote minerals are a relict from an earlier, hotter regime and the liquid- dominated reservoir evolved into a vapor-dominated system (Browne, 1978). Epidote can therefore be important in reconstructing the temperature evolution.

The process of hydrothermal alteration is also very important in the formation of a sealing layer. Cap rock is formed by secondary clay minerals, which naturally have a low permeability. The formation and distribution of these clay minerals is also controlled by the reservoir temperature (Browne & Ellis, 1970, Muffler & White, 1969, Steiner, 1968). At lower reservoir temperatures ranging from 80°C to approximately 150°C, kaolinite and smectite are the dominantly formed clay minerals (Figure 7). Minerals from the smectite group, such as montmorillonite, become more important with increasing temperatures. As the temperatures approach 200°C, montmorillonite becomes interstratified with illite. Above 220°C, illite and chloride usually form the typical assemblage of clay minerals (Browne, 1978). Whether specific geothermal systems show the temperature dependent clay mineral envelope, is also strongly dependent on the chemical composition of the thermal fluids. Therefore, conclusions regarding the temperature based on the clay mineral assemblage should be treated with caution.

The chemistry of these thermal fluids depends on the interaction of the fluids with the surrounding rock. Studies on the alteration in geothermal fields have recognized the import control of permeability on the reactions between rocks and the reservoir fluids (Browne, 1978). Furthermore, there is a close relationship between the fluid chemistry and the mineralogy of the source rock. The dissolution of chemical components from the reservoir rock into the geothermal fluids depends on the solubility of these components. This solubility is in turn controlled by the fluid pressure and temperature, since these properties alter the intermolecular forces between the solver and the solvent. Fluid pressures are generally low (Browne, 1978): in liquid-dominated fields, the pressures are close to hot hydrostatic, while in vapor-dominated systems, the fluid pressures are typically well below hydrostatic (White et el., 1971). Clays, such as kaolinite and montmorillonite, are typically more abundant in rocks affected by steam (Browne, 1978).

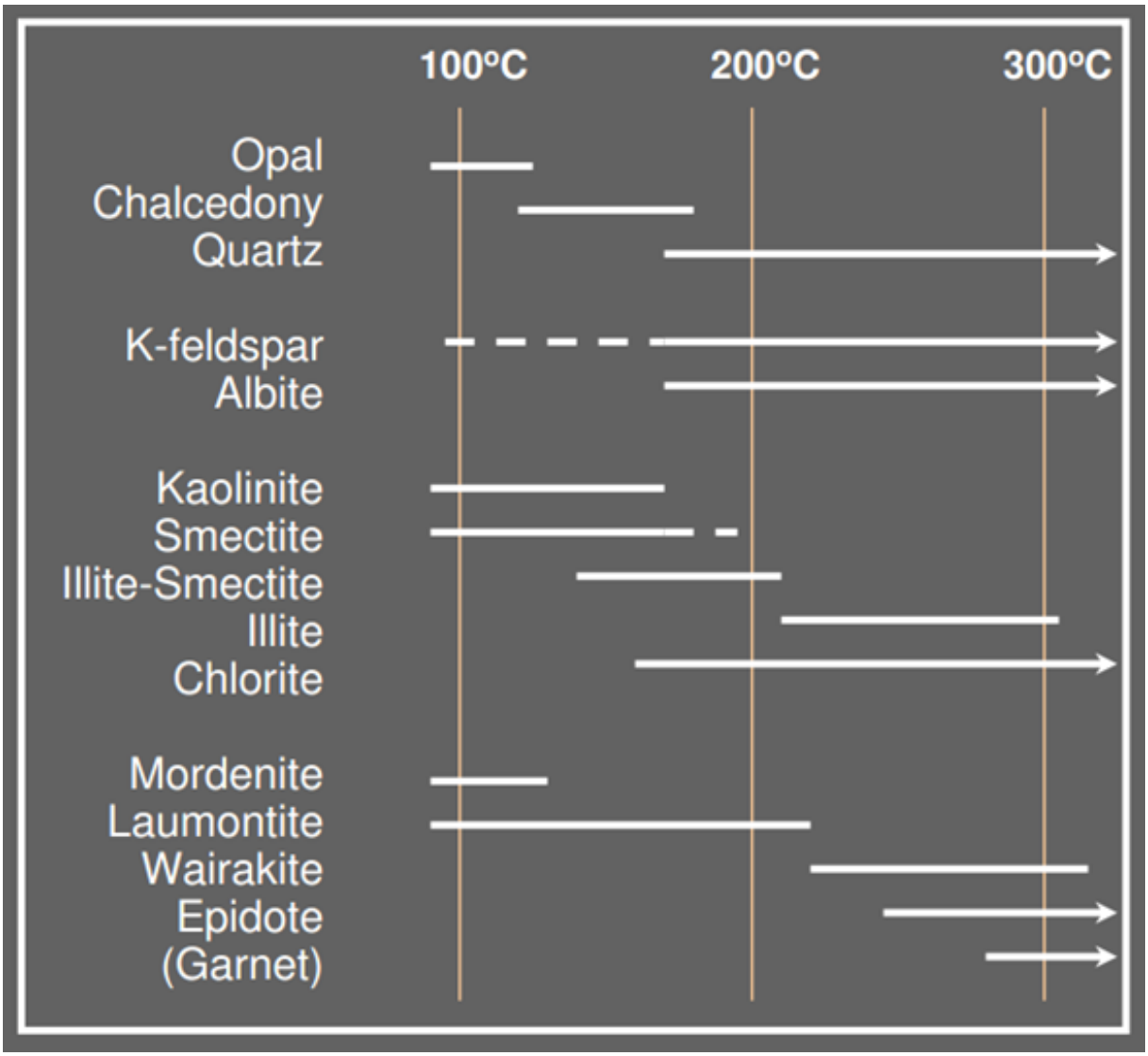

Figure 7 List of secondary minerals and the range of temperatures at which they occur (Bignall, 2010)

4 Geothermal manifestations

There are many geothermal field manifestations of varying type in the Patuha, such as hot springs, fumaroles and kawahs (*kawah* is the Indonesian word for crater). The type of manifestations, its temperature and chemical content holds much information about the geothermal reservoir.

4.1 Surface manifestations in the Patuha area

The type of surface manifestation and their location can be related to geological structures and up- and outflow zones of the geothermal system. In general, an upflow zone is associated with "steaming ground" or fumaroles, while outflow zones are associated with hot springs (Figure 2). In the next Paragraph, the different types of geothermal manifestations at the Patuha area will be described.

4.1.1 Type of geothermal manifestations

Crater lakes

A crater lake can be formed when a depression as a result of a volcanic eruption is filled with water by precipitation. If such a lake is formed above an active volcano, the lake water is often acidic and saturated with volcanic gases. The water will become cloudy with a distinct smell and greenish color.

Hot springs

A hot spring is a spring of geothermally heated groundwater that emerges from the surface. The groundwater rises up from the subsurface through high permeability zones in the subsurface, such as cracks and fractures. There are several different definitions of a hot spring, mainly based on temperature. In this thesis, a hot spring is a geothermal spring with temperatures above 50°C. When the temperature of outflow waters are below this value, the geothermal springs are revered to as warm springs (25°C-50°C) or cold springs (< 25°C).

Fumaroles

A fumarole is an opening in the Earth's crust which emits steam and several volcanic gases, such as carbon dioxide, sulfur dioxide, hydrochloric acid and hydrogen sulfide. The pressure drop causes the water to turn into steam, when superheated water emerges from the ground. Fumaroles usually originate along small cracks and fractures in areas where magma or igneous rocks occur at shallow depth. Gases released from these rocks interact with the groundwater system and results in thermal springs and gas vents. Fumaroles differ from hot springs, only because the water is turned into steam as it reaches the surface. This implicates larger subsurface temperatures or a larger pressure drop. Fumaroles are sometimes revered to as steaming ground.

Mudpots

With limited availability of water, surface manifestations as an acidic hot spring or fumarole can turn into a mudpot. Spots of boiling mud, with usually a white or grayish color, can be formed when the little water that is available rises to the surface and comes in contact with fine particles, such as volcanic ash and clay.

4.1.2 Distribution and classification of the geothermal manifestations at Patuha

The distribution of the surface manifestations is given in Figure 12. The kawahs are mainly situated near the high peaks, such as Mt. Patuha and Mt. Urug. Kawah Putih (*putih* means white in English) is a crater lake which is situated on the southern side of the top of Mt. Patuha (Figure 8). There are several other surface manifestations near the lake, mostly fumaroles with measured fluid temperatures of approximately 86°C.

Figure 8 Crater lake at Kawah Putih

Kawah Ciwidey is located in the eastern part of the concession area, close to Mt. Urug, and is dominated by fumaroles. There are several high temperature hot springs (up to 92°C) present at this location (Figure 9).

Figure 9 Steaming ground at Kawah Ciwidey

Kawah Cibuni is located in the TEKNOSA concession area. This area is also marked by the presence of steaming ground and high temperature hot springs. At this kawah there are also several mudpots (Figure 10). Approximately one kilometer southwest of Kawah Cibuni are the springs of Cisaat. The temperatures of these cold springs are 22-24°C.

Figure 10 Steaming ground at Kawah Cibuni

The springs of Barutunggul (Figure 11) and Rancawalini are located close to the northern boundary of the concession area. The first can be classified as warm springs since the measured temperatures are between 42°C and 45°C.

Figure 11 Hot springs at Rancawalini

The temperatures at the springs of Rancawalini are somewhat higher (~50°C) and can therefore be classified as hot springs. The Cimanggu hot springs are more south and closer to Mt. Patuha and Kawah Putih. At these springs, temperatures ranging between 65°C and 83°C were measured. South in the area, the warm springs (35°C) of Cibunggaok as well as the cold springs (~20°C) at Kawah Tiis are present.

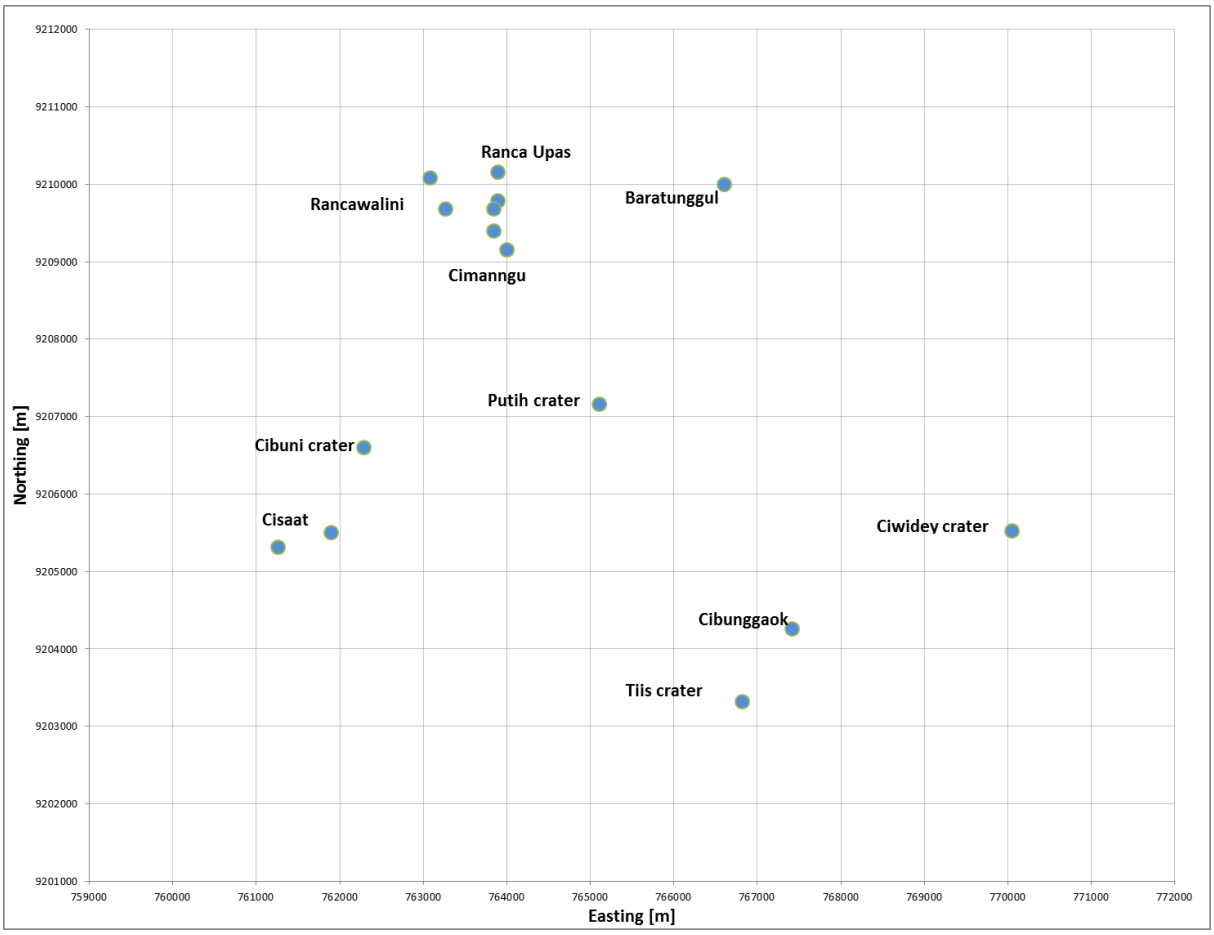

Figure 12 Distribution of surface manifestations.

4.2 Composition of the geothermal waters from surface manifestations

The chemical data from these manifestations gives an indication about the origin of the geothermal fluids. The chemical composition and acidity reflects the flow path and fluid-rock interaction of these surface waters.

4.2.1 Chemistry of geothermal waters

Following Nicholson (1993), geothermal waters can be classified according to the dominant anion. In general, chloride fluids are the most common fluid type at high temperature geothermal systems. These fluids originate at large depth. Others geothermal fluid type, like sulphate and bicarbonate waters, can generally be derived from these chloride fluids as a consequence of chemical or physical processes.

Since the chloride fluid type is associated with deep geothermal fluids, surface manifestations with large concentrations of chloride are assumed to be fed directly from the deep reservoir. These waters are directly associated with high permeable zones in the geothermal system, like for example a fault.

Sulphate waters are formed by condensation of geothermal gases into oxygenated groundwater. Due to the solubility of these gases, they are separated from the chloride waters by boiling at depth. Sulphate

waters are found at the margins of the geothermal field, away from the main upflow zone. They are generally found near the surface in perched water tables and above boiling zones. However, when there is a fault present, the fluids can penetrate to larger depths where they are heated and will play an important role in alteration processes or dissolve in chloride fluids again.

Sulphate is the main anion in these waters and is formed by the oxidation of hydrogen sulphide as described by the following reaction equation:

$$H_2S(g) + 2O_2(aq) = 2H^+(aq) + SO_4^{2-}(aq)$$

In combination with the condensation of carbon dioxide this creates highly acidic waters, due to the production of protons. This reaction equation is:

$$CO_2(g) + H_2O(l) = H_2CO_3(aq) = H^+(aq) + HCO^{3-}(aq) = 2H^+(aq) + CO_3^{2-}(aq)$$

The oxidation process resulting in these acid sulphate waters can reach a minimum pH of 2.8 (Nicholson, 1993). Geothermal waters with a significantly higher acidity are likely to have been in direct contact with magmatic gases. Chloride is only present in small amounts and bicarbonate can even be absent, since in very acid waters the dissolved carbonate is lost from the solution as carbon dioxide. These sulphate waters will discharge at the surface as (boiling) mud pools, steaming ground or acid hot springs.

When the sub-surface waters are poorly-oxygenated, the condensation of steam and gas can result in neutral bicarbonate-sulphate waters. Due to a lack of oxygen, the oxidation of hydrogen sulphate cannot set through, therefore limiting the production of protons to the condensation of carbon dioxide. Since these protons are consumed by the reaction of these waters with the surrounding rocks in shallow reservoirs or during lateral flows, bicarbonate waters are usually of near neutral pH. Sulphate is still present in variable amounts, but the amount of chloride is negligible. (Mahon et al., 1980). This is because chloride is not present in the steam or gas phase. As well as sulphate waters, bicarbonate waters are found at the margins of the system.

There can also be a mixture of the different water types resulting in for example sulphate-chloride waters or dilute chloride-bicarbonate waters. The pH of these waters is respectively 2-5 and 6-8. The formation of sulphate-chloride waters can however also be explained by several other processes: a) near surface discharge and oxidation of H2S in chloride water. b) near-surface condensation of volcanic gases into meteoric waters. c) condensation of magmatic vapor at depth. d) passage of chloride fluids through sulphate bearing sequences or lithologies containing native sulphur. Mixing of chloride and sulphate waters is however probably the most common process (Nicholson, 1993).

The geothermal waters can also be classified by using a ternary plot (Figure 13). This plot uses the relative proportions of chloride, sulphate and bicarbonate to describe the geothermal waters according to the above classification.

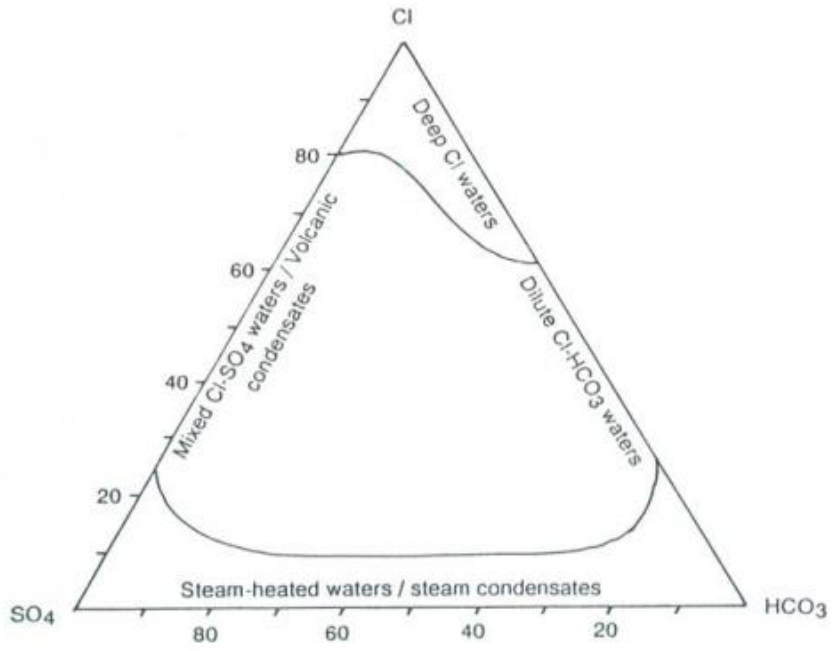

Figure 13 Ternary plot used to classify geothermal waters (Nicholson, 1993)

4.2.2 Composition of the surface manifestations at the Patuha field

The composition of the geothermal waters of the surface manifestations is known and their chemical content is listed in Table 4. The exploratory work on the composition of the surface manifestations was conducted by PERTAMINA in 1983 (Layman et al., 2003)

Table 4 Chemical composition (concentration in mg/kg) of water in the Patuha geothermal field (West JEC, 2007)

		Date	Temp °C	pH		TDS	Na	K	Ca	Mg	Cl	SO_4	HCO_3	CO_3	Li	Sr	B	F	As	SiO_2
				Field	Lab															
Barutunggul	ws		42		6.3		124.2	38.8	286	89	99	701	649		0.31		9.4	0.24		130
Barutunggul	ws	5/10/1997	45	5.84	7.15	2080	144.66	42	262.09	118.49	458.8	485.35	393.2	<2.0	<0.020	0.359	10.16	0.141		161.47
Cibunggaok	ws		35		6.8	307	20	5.8	26	8	8	63	80		0.04		0.6	0.15		95
Cibunggaok	ws	5/12/1997	35	6.6	7.62	335	16.55	6.44	30.68	8.43	7.97	70.1	70.53	<2.0	<0.020	0.062	0.156	0.103		123.97
Cimanggu	hs				7.52	1485	126	50	116.37	64.41	260.51	275	385.1		1.33		6.73		0.17	199
Cimanggu	hs		83		6.72		62.5	13	13	5	14	7	239		0.05		2.6	0.25		188
Cimanggu	hs		65		6.81		107.6	51.9	109	75	266	284	264		0.28		5.6	0.25		180
Cimanggu	hs	5/8/1997	75	6.15	7.23	670	63.91	14.3	37.76	12.66	18.68	20.97	299.8	<2.0	0.041	0.854	0.829	0.196	0.044	199.9
Cisaat	cs	5/9/1997	24	2																
Cisaat	cs		22		2.02		9	7.5	30	20	4	1930	37		0.004		0.05	0.11		113
Kawah Cibuni					3.71		22.37	10.98	63.48	41.49	7.24	750	0		0.47		0.49		0.12	230
Kawah Cibuni	cw	5/9/1997	21	7.23	8.47	195	8.75	2.89	14.33	8.98	12.68	37.61	59.26		<0.020	0.041	<0.20	0.054		50.4
Kawah Cibuni	fw	5/9/1997	92	2	2.31	1160	8.13	3.86	8.07	9.05	1.32	885.23	<2.0		<0.020	0.38	0.166	0.236	0.0142	239.8
Kawah Cibuni	hp		85		2.46		42.3	22.1	294	47	1	1208	0		0.43		0.05	0.23		180
Kawah Cibuni	hs		90		2.49		97.8	56.4	190	22	384	385	0		0.62		1	0.53		80
Kawah Cibuni	m		92	2	2.52	638	5.92	3.05	11.87	7.26	2.74	485.09	<2.0	<2.0	<0.020	0.065	<0.20	0.144		121.88
Kawah Ciwidey	hs	5/7/1997	92	6.35	4.19	237	8.11	3.32	9.74	1.51	0.348	59	<2.0	<2.0	<0.020	<0.020	<0.20	0.477		154.18
Kawah Ciwidey	cw	5/7/1997	20	7	4.02	24.5	0.69	0.23	11.19	0.84	0.505	10.75	<2.0	<2.0	<0.020	<0.020	<0.20	0.074		10.2
Kawah Ciwidey	f	5/7/1997	85	2.57											<0.020				<0.005	
Kawah Ciwidey	hp		87		6.83		5.2	2.3	10	6	<1	40	36		0.01		0.05	0.32		98
Kawah Ciwidey	hs		69		2.75		21.5	14	90	20	<1	442	0		0.2		0.05	0.22		18
Kawah Putih					2.66		50.85	42.04	65.1	333.5	9909.3	830	0		1		86.97		0.04	153
Kawah Putih	f	5/8/1997	86	0.56											<0.020				<0.005	
Kawah Putih	lw		30		1.01		1502	1322	4802	2026	17008	3102	0		0.02		49.3	1.8		260
Kawah Tiis	cs		22		2.36		41.3	10.9	274	222	7	6613	0		0.85		0.05	0.62		500
Kawah Tiis	cw	5/8/1997	18	5	5.65	68.5	1.94	0.838	2.78	1.01	1.35	8.68	31.65	<2.0	<0.020	<0.020	<0.20	<0.025	<0.005	20.2
Rancawalini					6.99		72.32	27.38	63.48	33.69	95.88	195	275.07		0.83		2.32		0.14	154
Rancawalini	hs		51		6.74		53.7	22.8	59	37	80	167	187		0.19		2	0.3		98
Rancawalini	hs	5/8/1997	50	6.15	8.03	906	61.55	23.81	52.62	47.98	117.5	179.17	254.5	<2.0	<0.020	0.09	2.21	0.292		166.73
Rancawalini II	ws	5/8/1997	49	6.2	7.32	899	62.73	24.38	81.09	43.94	111.78	167.1	227.11	<2.0	0.101	0.11	2.27	0.279		177.87
Rancawalini II	ws		44		6.87		61	20	46	28	80	150	149		0.26		7.5	0.26		97

ws = warm spring hs= hot spring cs = cold spring cw = cold water f = fumaroles water hp = hot pool m = mudpot lw = lake water Temp. = temperature Lab. = laboratory

For Barutunggul, data of two water samples are available. In one sample, SO42- and HCO3- are the dominating anions, while in the other sample Cl- is present in equal concentrations. The two samples at Cibunggaok have SO42- and HCO3- as the main anions, though the overall concentration of chemical components in these samples is relatively low. At the hot springs in Cimanggu, HCO3- is the main anion, although two water samples show Cl-, SO42- and HCO3- in almost the same concentration. In Rancawalini, main anion is HCO3- although the anions of SO42- and Cl- are also quite abundant. For all these hot springs, the pH is close to neutral, varying between 6.3 and 8.0.

The pH is highly acidic for the fumaroles at Kawah Cibuni and Kawah Ciwidey (respectively 2 and 2.57). The main anion in these waters is SO42-. The fumarolic waters at Kawah Putih have an extremely low pH (<1) and even the lake water of Kawah Putih has a very low measured pH of 1.01. The lake water contains very high concentrations of chemical components, mainly Cl- (17008 mg/kg) and SO42- (3102 mg/kg). There is no HCO3- found in the lake water at Kawah Putih. Based on the high acidity and the chemical composition of the fumarolic waters from Kawah Putih, it is likely that these fluids have been in contact with active magmatism. In combination with the measured high temperatures at this surface manifestation, Kawah Putih can be considered as an upflow zone of high temperature geothermal fluids. The measured temperatures of the fluids at Kawah Ciwidey and Kawah Cibuni are similar to those at Kawah Putih. Combined with the high acidity, it is also possible that there is an upflow zone present at these locations. However, it is also possible that the high temperatures of the fluids are a result of lateral flow from the upflow zone at the Kawah Putih, since the fluid composition differs from that at the Kawah Putih.

Based on the composition of these waters, ternary plots of the main surface manifestation of the Patuha field are constructed, including Kawah Putih, Kawah Ciwidey, Kawah Cibuni, and the hot springs of Rancawalini, Barutunggul and Cimanggu (Figure 14).

Based on these plots, the geothermal waters at Kawah Putih can be classified as deep chloride waters. This confirms the assumption that there is a highly permeable zone situated beneath this crater lake. In combination with the heat source from the Mt. Patuha volcano, it can be concluded that there is a direct upflow of high temperature geothermal fluids at this location. At Kawah Ciwidey, the geothermal waters can probably be best described as sulphate waters. Since chloride is only present in small amounts (<1 mg/kg). This is most probably caused by mixing of chloride and sulphate waters, although the condensation of magmatic gases could have contributed to the chemical content of the fluids. The composition of the geothermal fluids at Kawah Cibuni is quite variable. There are samples that show sulphate waters, but also samples that are a mixture of different types of fluids. The geothermal fluids at Kawah Cibuni also discharge as different types of surface manifestations. There is no unambiguous explanation given for this variation in manifestation type and chemical content of the fluids in this area. However, it is likely that the influence of the mixing of the geothermal waters with surface water and groundwater varies within this small area.

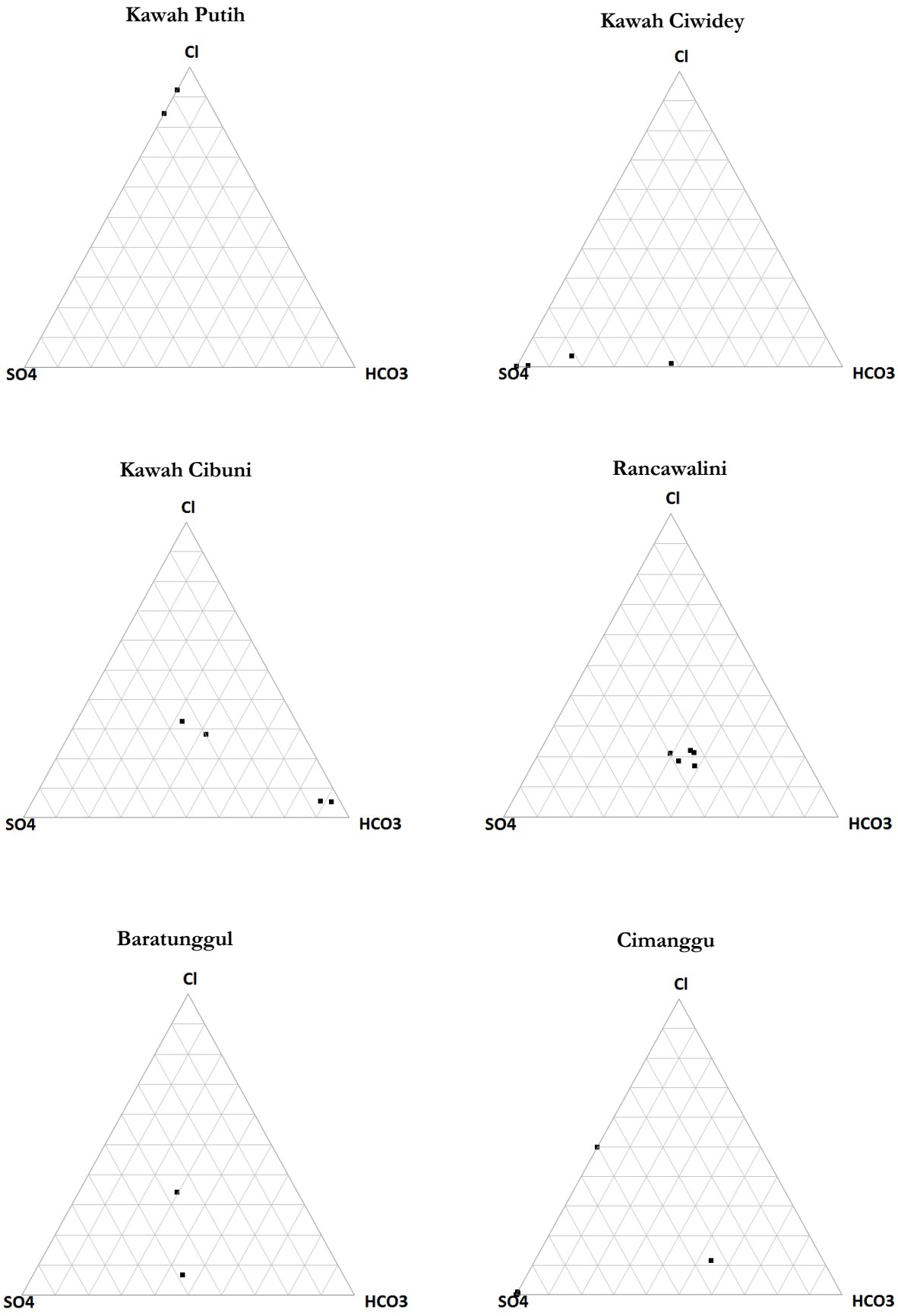

Figure 14 Ternary plots of the chemical composition of the geothermal fluids at six surface manifestations in the Patuha area

The ternary plots of the different hot springs do not show a clear classification of the fluid type, since the concentrations of the main chemical components do not show a dominant anion (Table 4). Therefore these waters are probably a mixture of the different fluid types. The samples of Rancawalini are all plotted in the central part of the ternary plot and it is therefore difficult to make a distinct classification based on this presentation. At Cimanggu, there are four samples of which two are also plotted in the central part of the diagram. The other two samples have very low concentrations of Cl-. HCO3- is in these samples the dominant anion. They are therefore classified as bicarbonate waters formed by steam heated waters or steam condensates. The hot springs at Barutunggul also show a varying content of the different samples. Of the two samples, one is plotted in the center of the diagram, which is therefore difficult to classify and the second sample is clearly plotted in the lower regions of the diagram. Therefore, the later has its origin in steam heated water. Since the concentrations of sulphate and bicarbonate are nearly similar, this sample is classified as bicarbonate-sulphate water.

5 Geophysical survey

5.1 Introduction

Geologic interpretation has been carried out by West JEC in an earlier stage. The outcome is expected to give a good understanding of the structural geology in the area. The interpretation is mainly based on the gravity lineaments derived from steep gravity changes and resistivity discontinuities. The location of the surface manifestations can be used to confirm the interpreted fault distribution. The following paragraphs are mainly based on the findings of West JEC as mentioned in the feasibility study for Patuha geothermal power development.

5.2 Gravity survey

Gravity data can be used to obtain the location of the large intrusive features and give an indication of the structural units in the area. A gravity map with a density correction of 2.2 g/cm^3 is given in Figure 15. In this map, several high anomaly areas can be identified (assigned with an H in Figure 15). These areas with a high-gravity anomaly can be associated with intrusive features (Battaglia and Segall, 2004). Therefore, these areas can be associated with a magmatic heat source.

The large scale west-northwest to east-southeast trending can also be recognized from the map. This is in line with the expectations based on the tectonic activity in the area (i.e. a volcanic belt with the same orientation as a result of the plate boundary between the Indo-Australian plate and the Eurasian plate, Paragraph 3.1)

Figure 15 Gravity map (West JEC, 2007)

In Figure 16, a correction for the regional trend of the gravity basement is applied. This limits the effect of the reflection of large scale, deeper geological structures on the map. Therefore, more local gravity features will be revealed on the map. This map is then used to estimate several gravity lineaments. These gravity lineaments, associated with steep gravity change, generally correspond with a geological structure (i.e. fault or lithological boundary) (West JEC, 2007).

Figure 16 Residual gravity map (West JEC, 2007)

5.3 Resistivity survey

A magnetotelluric (MT) and time-domain electromagnetic (TDEM) survey are carried out in order to obtain the resistivity values of the subsurface. The resistivity is inversely related to the electrical conductivity. The resistivity can be associated with the permeability, since rocks with a high conductivity are typically associated with (low permeability) alteration zones. When volcanic rocks come in contact with geothermal fluids, clay minerals can form due to the alteration processes (Paragraph 3.3). This process is controlled by thermodynamic properties of the fluid and surrounding rock. Clay minerals are very good conductors due to their internal structure, and therefore show a low resistivity. Clay minerals generally have a very low permeability and can therefore be expected to act as cap rock.

During this study it is assumed that the top of the conductor (based on resistivity values less than 10-15 ohm.m) is related to the top of the cap rock. Figure 17 shows that the cap rock appears closest to the surface at Kawah Putih. This is consistent with geochemical data from the surface manifestation. Clay minerals alter closer to the surface due to higher temperatures near the upflow zone.

The map also shows a similar pattern of low resistivity values around Kawah Ciwidey and Kawah Cibuni. Combined with data from the fluid chemistry of the two Kawahs (Paragraph 4.3), it could be possible that there are multiple upflow zones present in the system.

Figure 17 Top of the conductor (Geosystem, 1995)

5.4 Interpretation of the structural geology

The gravity and resistivity data is used to give an estimation of the geological structures in the main area of the Patuha field. Eight faults were directly derived from this data (Table 5), as can be read in the feasibility report by West JEC (2007). Two more faults (F9 and F10) are predicted based on temperature distribution (higher subsurface temperatures are measured on the northwestern side of the fault compared to the southeastern side of the fault) and the arrangement of volcanic cones from Mt. Patuha to Mt. Patuha South (West JEC, 2007).

Table 5 Estimated faults (by West JEC, 2007)

Fault number	Trending	Dipping to …	Estimation based on …
F1	NW-SE	Southwest	Gravity lineament G2
F2	NW-SE	Southwest	Gravity lineament G3
F3	E-W	North	Gravity lineament G4
F4	NE-SW	Southeast	Gravity lineament G11
F5	NE-SW	Southeast	Gravity lineament G8
F6	NE-SW	Southeast	Gravity lineament G10
F7	NE-SW	Southeast	Gravity lineament G6
F8	E-W	North	Gravity lineament G7
F9	NE-SW	Northwest	Temperature distribution
F10	NNW-SSE	East-northeast	Arrangement of volcanic cones

Figure 18 shows a map of the established fault system. The West JEC report also provides several cross-sections of the Patuha geothermal field (Appendix A). These show the locations and the dipping angle of the faults mentioned in Table 5. The dipping angles illustrated in these cross-sections are rough estimations. These are mainly based on the general assumption that faults in volcanic regions which are related with island-arc systems have a dipping angle between approximately 75° and 90° (West JEC, 2007). The cross-sections also show the presence of different rock types, like Quaternary and Neocene volcanic rocks, intrusive rocks and argillized impermeable layers. These are derived from the distribution of low resistivity zones and borehole data (borehole data is presented in Paragraph 7.3). As can be seen in the cross-sections, the argillized layer approximately follows the isotherms. The bottom of the layer is situated around 200 °C, and the upper part is approximately around 50 °C.

Figure 18 Distribution of estimated faults (West JEC, 2007)

5.5 Relation to surface manifestations

There is a clear relationship between the established faults and the presence of surface manifestations (Figure 19). Surface manifestations are the result of fluid flows towards the surface. This generally occurs along specific zones of high permeability. Volcanic rock naturally has a very low permeability, so these zones of high permeability must be related to the structural geology of the area.

Figure 19 Relationship between geothermal manifestations and estimated faults

6 Synopsis

6.1 Introduction

In order to develop a conceptual model, it is necessary to combine all the available data for a complete overview of the reservoir of interest. Important reservoir properties that should be determined are the distribution and thickness of the cap rock, the up- and outflow zones of geothermal fluids and the approximate location of the heat source. Finally, the size and temperature distribution of the reservoir should be indicated.

6.2 System properties of the Patuha geothermal resource

6.2.1 Up- and outflow zones

Data from geothermal manifestations, like the type of manifestation, the obtained temperatures and chemical composition of the fluids, can be used to estimate the location of up- and outflow zones. The chemical composition gives an indication on the type and origin of the geothermal fluids. Based on this data, the geothermal fluids at Kawah Putih are classified as deep chloride waters. This suggests that there is a highly permeable zone beneath this location. Therefore it is thought that the main upflow zone is located at Kawah Putih. There are also indications that around Kawah Cibuni and Kawah Ciwidey a second and third upflow zone is present. However, the similar properties of these surface manifestations can also be a result of lateral flow from one central upflow zone at Kawah Putih. The latter is more likely since the geothermal waters at these surface manifestations are classified as sulphate waters or a combination of different types of geothermal waters.

The hot springs of Barutunggul and Rancawalini are regarded to be outflow zone based on the chemical analysis and type of manifestation (Paragraph 4.2). The presence of these outflow zones indicate that around these locations the boundaries of the reservoir are reached.

The chemical composition of the geothermal fluids can give an indication on the flow path of these fluids, since the composition is mainly controlled by the interaction of the fluids with the surrounding rock. Another important factor is the solubility of the components, which depends on the temperatures and pressures of the system. Sulphate and bicarbonate are easily transmitted into the gas-phase. Water samples that contain high amounts of sulphate and bicarbonate are therefore thought to be formed by condensation of steam and gas, while chloride waters originate from large depth.

6.2.2 Cap rock

The cap rock is characterized by the presence of argillic clay minerals. Therefore resistivity analysis can be used to determine the depth and location of this layer. The internal structure of the clay minerals causes a large electrical conductivity and therefore shows a low resistivity. Especially the surveys which show low resistivity values are important to determine the dimensions of the cap rock. At Kawah Putih, the cap rock nearly reaches the surface. At Kawah Cibuni and Kawah Ciwidey, the cap rock is also obtained at

relatively shallow depth. Near the boundaries of the system, the presence of cap rock is less dominant and also present at larger depths. Faults cause a zone of high permeability in the cap rock. The surface manifestations are a clear result of these high permeability zones. Fault zones are also the most probable flow paths of geothermal fluids, since the natural permeability of volcanic rock is very low.

6.2.3 Reservoir Size

For the determination of the reservoir boundaries several parameters can be used, like for example the temperature and the permeability. Since none of these parameters are quantified at this stage, only indirect information on these parameters can be used to define the boundaries. The best indication can be given by the location of the different hot springs in the area. Since the presence of these surface manifestations implicate fluid flow towards the surface, the permeability at depth can be assumed to be sufficient for the production of geothermal fluids. Therefore, the hot springs are assumed to mark the outside boundaries of the reservoir. It is assumed that beyond these hot springs, the volcanic rock is relatively impermeable. The flow outside the reservoir boundaries is therefore assumed to be limited.

6.2.4 Temperature distribution

Measurements of the temperatures of the fluids at the surface manifestations show that at the Kawah Putih, Kawah Cibuni and Kawah Ciwidey the temperatures are the highest (> 80 °C). Therefore it is likely that the subsurface temperatures are also higher at these locations. At this stage, these surface measurements are the only source of data for the temperature in the reservoir. Well measurements are necessary to obtain a more exact subsurface temperature distribution (Chapter 7). Alteration minerals identified in well cores can give an indication on the subsurface temperatures, since most of these minerals are usually formed within a certain temperature range. The occurrence of epidote for example is an indication for reservoir temperatures above 240 °C. Pressure profiles from the wells can give an indication of the fluid type that is present in the well. Since the Patuha system is vapor-dominated, the temperatures are probably close to 240°C, since this is the temperature of the maximum enthalpy of steam. The best method to obtain the subsurface temperatures is to measure them directly as part of the drilling program.

6.2.5 Steam cap

Since the Patuha field is vapor-dominated, it is also important to know the lateral and vertical extension of the steam cap. The lateral extension can best be determined by pressure and temperature data form the wells (Chapter 7). A constant pressure and temperature with depth is an indication for a vapor-dominated zone. Since temperatures in vapor-dominated systems can never exceed 240 °C, alteration minerals that are associated with higher temperatures can be an indication for liquid-dominated conditions. The presence of these minerals can also be a relic, and therefore represent an earlier stage of the system. Whether there is a deep liquid layer below the steam zone can also be identified from well measurements, provided that the wells reach this level.

7 Well data

7.1 Exploratory drilling program

The initial exploration of the Patuha field was conducted by PERTAMINA in 1983. Part of this exploratory work was to obtain the thermal gradients from several shallow wells (up to 200 meters deep). These holes were drilled near the thermal features: one in the vicinity of the three fumarolic areas and one near the thermal springs in the northern part of the concession area. The exploration was taken over by Patuha Power Ltd. (PPL) in 1994. This affiliate of CalEnergy Co. started an extensive drilling program in 1996. During a period of two years, 17 deep temperature gradient holes and 13 production test wells were drilled. Flow testing in these test wells indicated that 9 out of 13 wells are productive (Layman et al., 2003). A combined steam production corresponding to 72.4 MWe was confirmed from these 9 wells (West JEC, 2007). The production wells are concentrated in the zone around Mt. Patuha and Mt. Urug. The locations of the drilling pads are given in Figure 20.

Figure 20 Location map of drilling pads (West JEC, 2007)

7.2 Geological well data

None of the wells in the Patuha field reaches the Tertiary sedimentary rocks. As can be seen in Figure 21 (a), the rocks found in the geothermal wells are volcanic rocks of Quaternary and Tertiary age. Some wells show the presence of (micro-) diorite intrusives that penetrate the volcanic sections (Layman et al., 2003). Several wells also show reddish, clay-rich horizons, which may represent paleosols. These zones have caused operational problems due to unstable hole conditions (Layman et al., 2003). In two wells, sulfur is identified at shallow depth (Figure 21 (b)), which is an indication for the presence of acidic fluids at these depths (West JEC, 2007).

Most of the wells also show weathering or alteration near the surface, which overlies a relatively thick argillic zone. In several wells, a silicified zone has been identified around 1200-1400 m above sea level. Below this zone, propylitization is recognized, as well as a continuous occurrence of epidote. The occurrences of propylitization and epidote are an indication that around this level (i.e. approximately below 1200 m above sea level), the temperature of hydrothermal alteration is over 200 °C (West JEC, 2007). The appearance of epidote coincide with reservoir temperatures below this 200 °C, which can be an indication for a collapse of several hundreds of meters of the isotherms of the system since the original formation of the epidote (Layman et al., 2003). In general, the well geology shows that the productive reservoir is made up of sequential volcanic rocks which have been altered by fracturing and water-rock interaction.

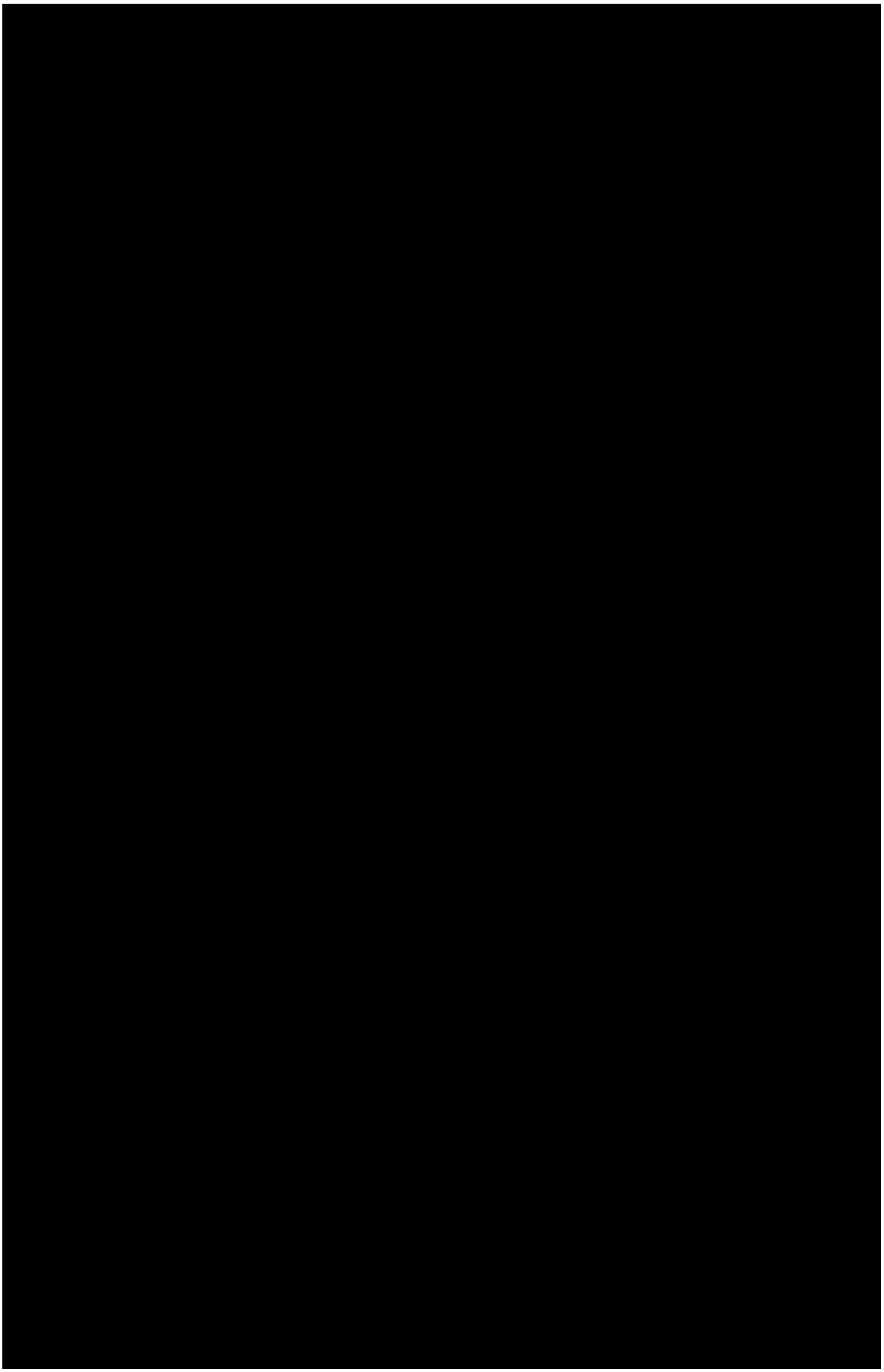

Figure 21 Well geology (West JEC, 2007)

7.3 Pressure and temperature profiles

The reservoir pressures and temperatures have been measured from 17 temperature core holes (TCH) and 13 full-sized wells. The pressure and temperature profiles which are expected to give the best representation of the natural state condition of the reservoir are selected (Figure 22 to Figure 25).

The profiles of the production test wells show a very low pressure gradient. Therefore, the pressure can be assumed constant over the entire reservoir. This is an indication for the presence of a steam zone. Several of these wells also show a deflection around 500 m.a.s.l.. This deflection may represent a liquid layer below the vapor zone, which is supported by the theoretical models (Paragraph 2.4). The pressure profiles of these wells show a typical hydrostatic gradient below this level (GeothermEx, Inc., 1997). However, since only a limited number of wells reach this depth, the existence and depth of a liquid layer remains a point of discussion. The presence of liquid in these wells could also be a result of condensation of the steam, or be a residual of the drilling fluids. Until more wells will reach this critical depth, there will be no certainty on the presence of a liquid layer below the vapor zone.

The temperature profiles of these wells show a large decrease in temperature between 1200 and 1500 meters above sea level. This zone corresponds to the impermeable argillic zone. This impermeable zone acts as a sealing layer for the transfer of heat, since the heat transfer in the reservoir is mainly controlled by convective flow through a permeable system.

The temperature differences in the steam zone (between 500 m and 1200 m.a.s.l.) are negligible. Therefore a constant temperature can be assumed in this depth range. It should be noted that this temperature is relatively low compared to other vapor-dominated reservoirs. Equilibrium temperatures in steam zones are generally near 240 °C, but the measured temperatures at Patuha range between 210 and 230 °C. There is no unambiguous explanation for the appearance of these lower temperatures at the Patuha system.

The pressure gradients of the TCH wells show that water is present in the wellbore (West JEC, 2007). Based on the occurrence of liquid water in these wells, it can be concluded that at the depth range of these wells, no steam zone is present. These drilling locations are therefore assumed to represent (the temperature and pressure distribution of) outside the vapor-dominated reservoir. The pressure and temperature profiles of these wells can therefore be used to estimate a general gradient. Based on Figure 22 and Figure 24 these gradients will be approximately 1 MPa/100 m for the pressure and 24.5 °C/100 m for the temperature.

The water levels in the TCH wells are identified at shallow depth and in some wells it even reaches up to the well head. This very shallow water level suggests that the rock around the wells have a very low permeability (West JEC, 2007). The downhole temperatures are very low in these wells. Since all the wells show a similar trend, it is not likely that these low temperatures are caused by mechanical problems with the wells (such as poor sementing). The presented profiles therefore are expected to represent natural conditions resulting from a downflow of cold water.

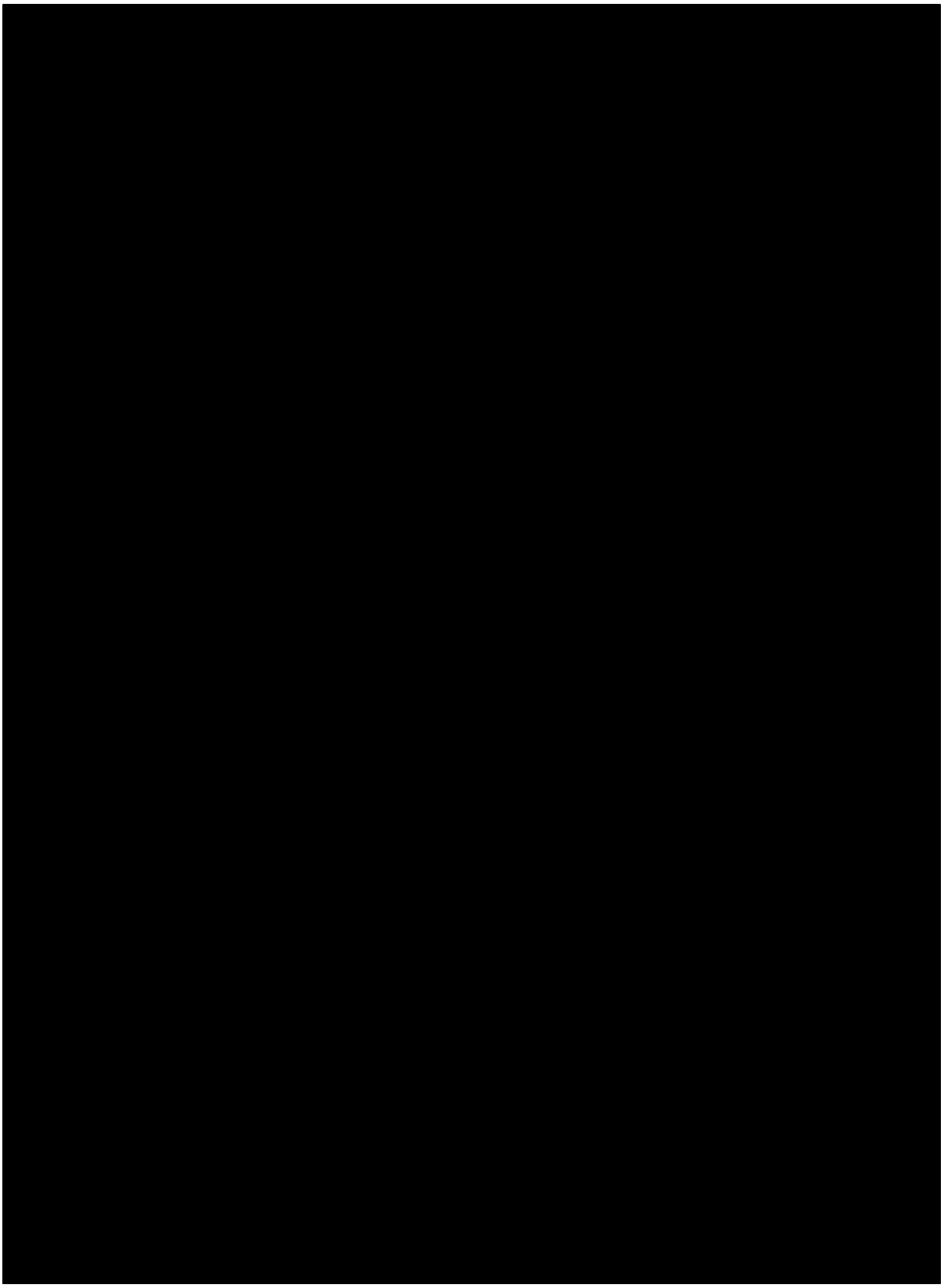

Figure 22 Pressure profiles of the temperature core holes

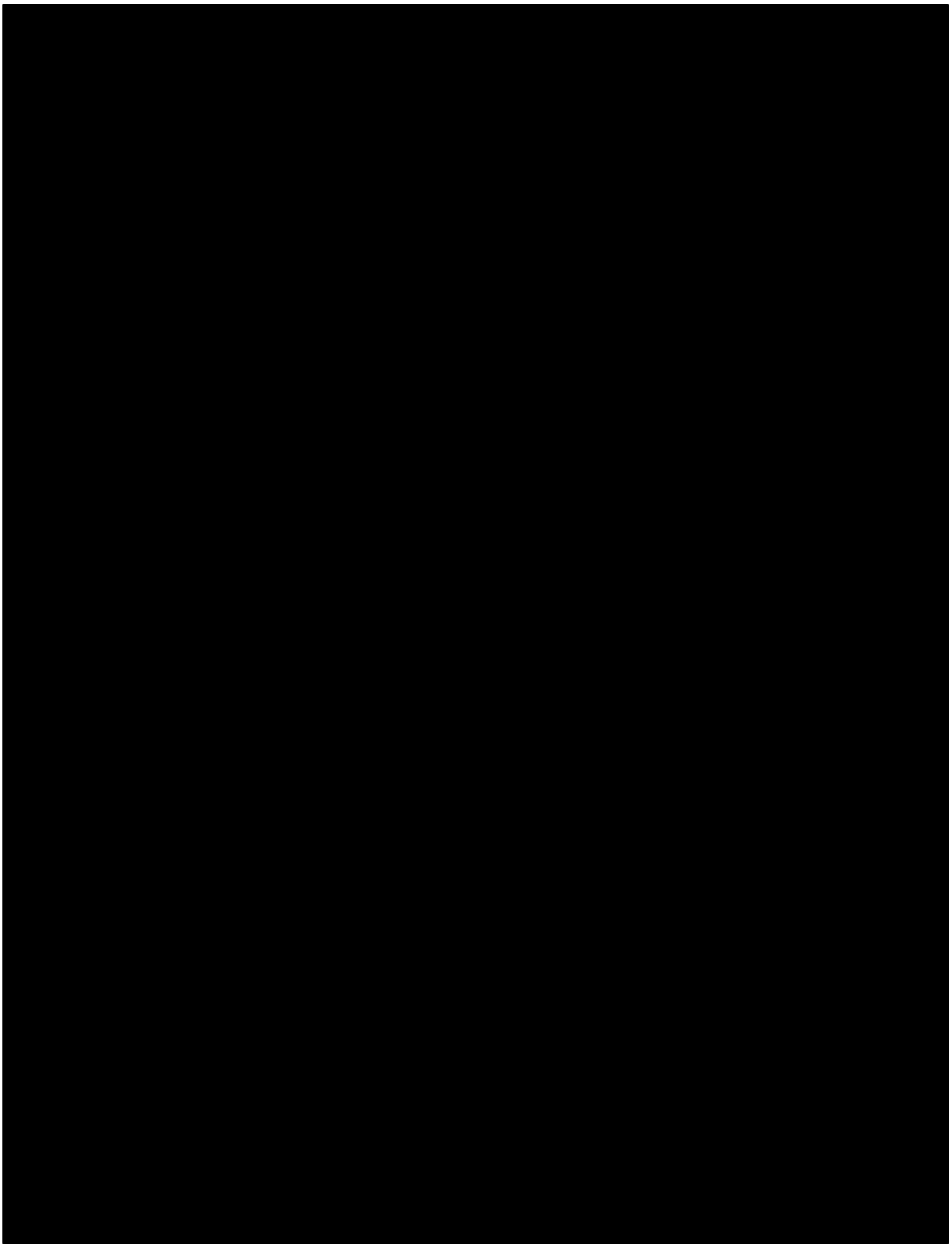

Figure 23 Pressure profiles of the production test wells.

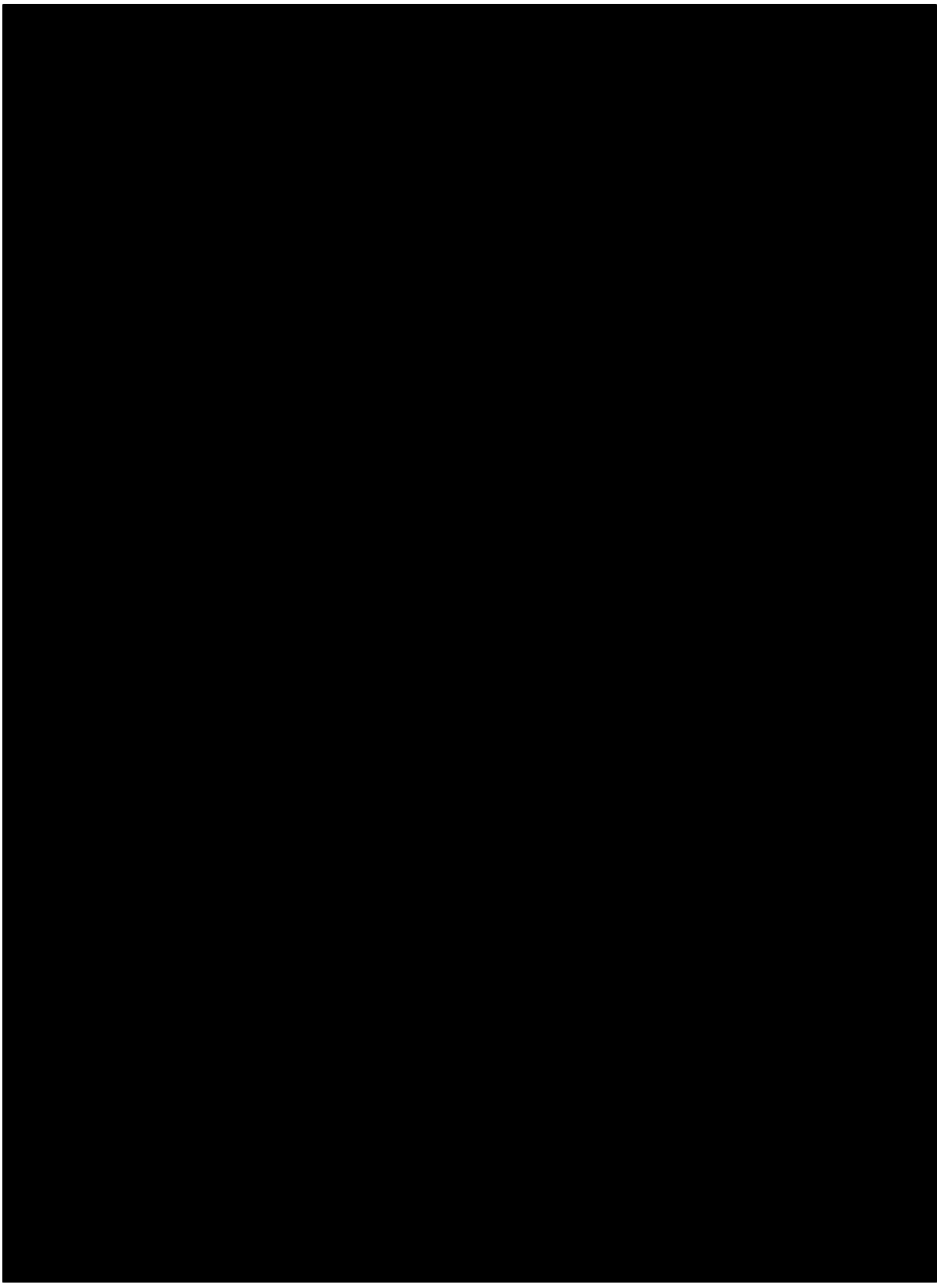

Figure 24 Temperature profiles of the temperature core holes

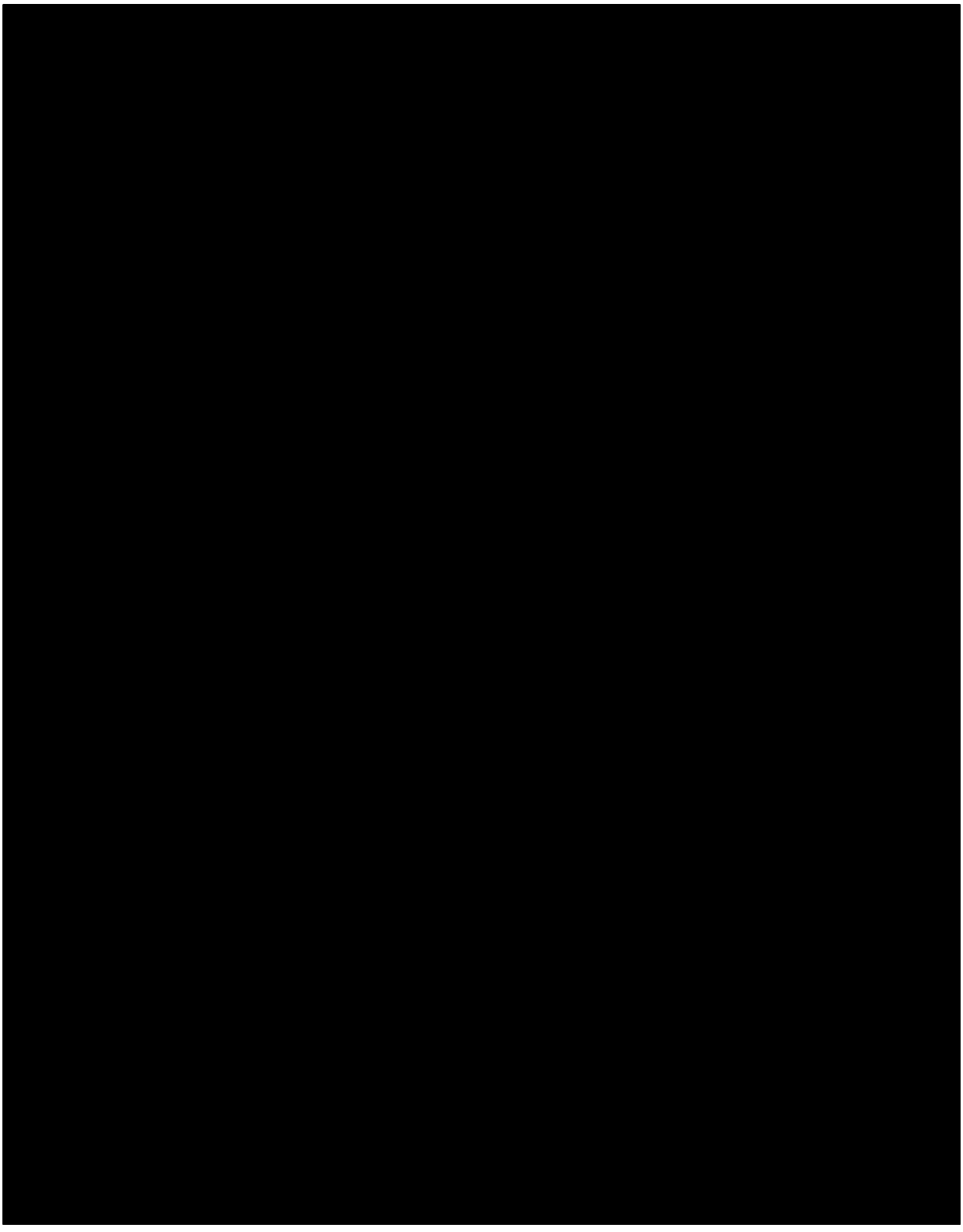

Figure 25 Temperature profiles of the production test wells.

7.4 Temperature distribution

The combination of the temperature logging data and the fault distribution is used to estimate the subsurface temperature distribution at three different depths (1200 m, 1000 m and 500 m.a.s.l.). The results are shown in Figure 26 to Figure 28. As can be seen in Figure 26 there are three major zones with temperatures above 200 °C, at relative shallow depth (1200 m.a.s.l.). These are around Mt. Patuha and extending to the Kawah Cibuni, corresponding mainly to faults F1, F5, and F10. At the western part of Mt. Urug there is a zone corresponding to F6 and at the northeastern part of Mt. Urug and the Kawah Ciwidey a major zone corresponds to fault F2. At 1000 m.a.s.l. the high temperature zones integrated to one large zone, extending from the Kawah Cibuni in the west to the Kawah Ciwidey in the east (Figure 27). This temperature zone is even larger at 500 m.a.s.l. (Figure 28)

Figure 26 Estimated temperature distribution at 1200 m above sea level (West JEC, 2007).

Figure 27 Estimated temperature distribution at 1000 m above sea level (West JEC, 2007).

Figure 28 Estimated temperature distribution at 500 m above sea level (West JEC, 2007).

8 Comparison of conceptual models

8.1 Introduction

In this chapter, two conceptual models of other authors will be discussed. In Paragraph 8.4, a new simplified conceptual model is presented which is used for the development of a numerical model. Since the conceptual model is developed with this specific purpose, the conceptual model is really straightforward and only shows the main features of the reservoir. This includes the main lithological features, the flow pattern, selected thermodynamical properties and surface temperatures.

8.2 Conceptual model by West JEC

Based on the available data, West JEC constructed a conceptual model of the Patuha geothermal system. This resulted in a plane view (Figure 29) and two sections (Figure 30) in which important features such as the upflow zones near Kawah Putih and Kawah Ciwidey and the dimensions of the steam cap and cap rock are illustrated.

As can be seen in the Figures presented of this conceptual model, the upflow zones clearly are associated with the fault zones in the area. In the cross sections, the presence of the cap rock and steam cap is visualized. The steam cap laterally spreads below the cap rock, which indicated the sealing function of the cap rock.

The cross sections also show that West JEC expects a steam separation point around 500 meters above sea level. Above this transition until about 1200 meters above sea level the reservoir is formed by a steam cap. Below this separation point there is a deep liquid reservoir in the vicinity of the fault zones.

Based on the chemical composition of the fluids at Kawah Putih, it is assumed that there has been contact with magmatic gases. It is presumed that these gases mainly flow upward along fault F10, because this interpreted fault follows the position of the volcanoes of Mt. Patuha and Mt. Patuha Selatan.

No specific research on the heat source has been carried out, but it is assumed that the heat source(s) can be related to the magmatic activity of Mt. Patuha, Mt. Patuha Selatan and also Mt. Urug. Therefore it is assumed that the heat source is located approximately below these volcanic cones.

Figure 29 Conceptual model of the Patuha geothermal field (plan view by West JEC, 2007)

Figure 30 Conceptual model of the Patuha geothermal field (cross sections by West JEC, 2007)

8.3 Conceptual model by Layman et al.

The conceptual model of Eric Layman (Figure 31) also assumes that the Patuha geothermal system is a vapor-dominated system on top of a deep liquid zone. The size of the reservoir is approximately 20 square kilometers. Besides these components, the centrally located magmatic plume is prominently present. The presence of this plume is derived by the chemical composition of Kawah Putih. Layman does not give any direct evidence of the presence of such a magmatic plume (there is no well data which confirms the theory). However, similar features have been intercepted at similar systems (Karaha-Telaga Bodas and Dieng) (Layman et al., 2003). This is used by Layman as a justification for his theory. The cross sections show that Layman assumes only a single heat source below Kawah Putih. The fumaroles at Kawah Ciwidey and Kawah Cibuni are supposedly the result of lateral flow from the central plume.

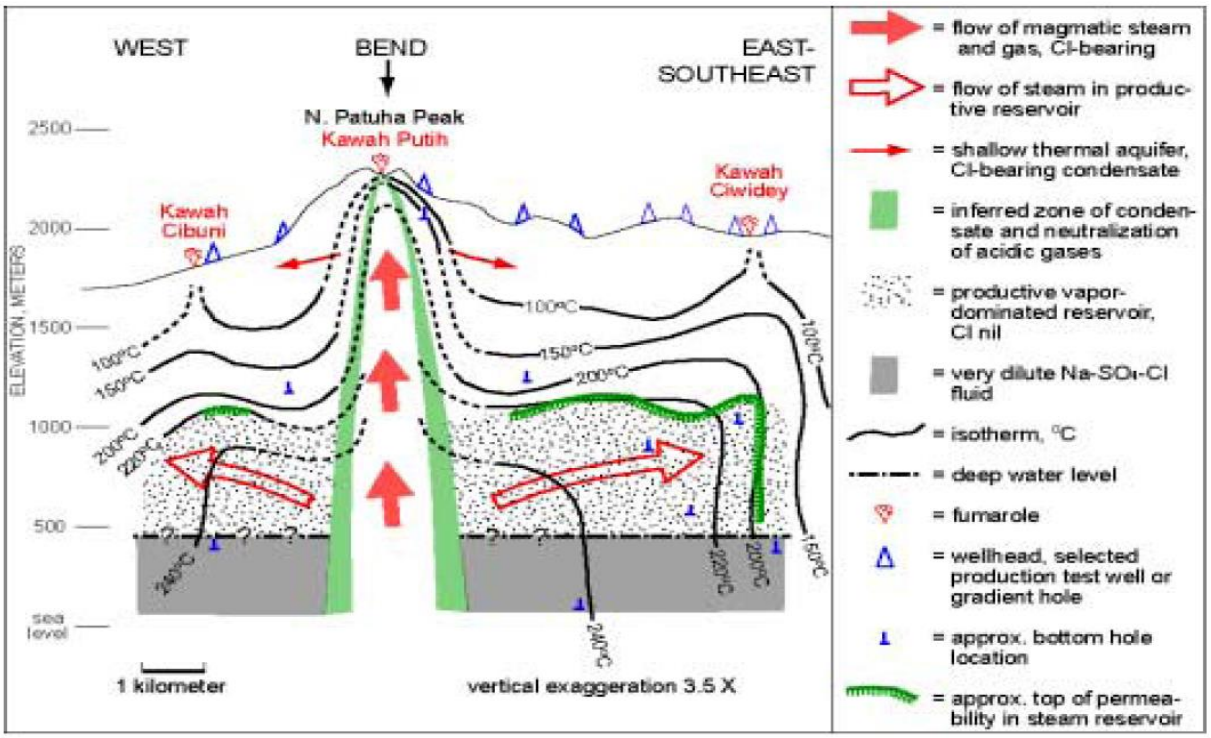

Figure 31 Conceptual model of the Patuha geothermal system (by Layman et al., 2003)

8.4 Conceptual model of the Patuha system

Figure 32 shows a simple and basic model of the Patuha vapor-dominated system. It contains the main lithological features, like the cap rock, the reservoir rock, the fault zones and the surrounding volcanic rock. Also, the most important surface manifestations are added to the model. The steady state temperature and saturation conditions are also given, as well as the temperature at the surface and at the kawahs.

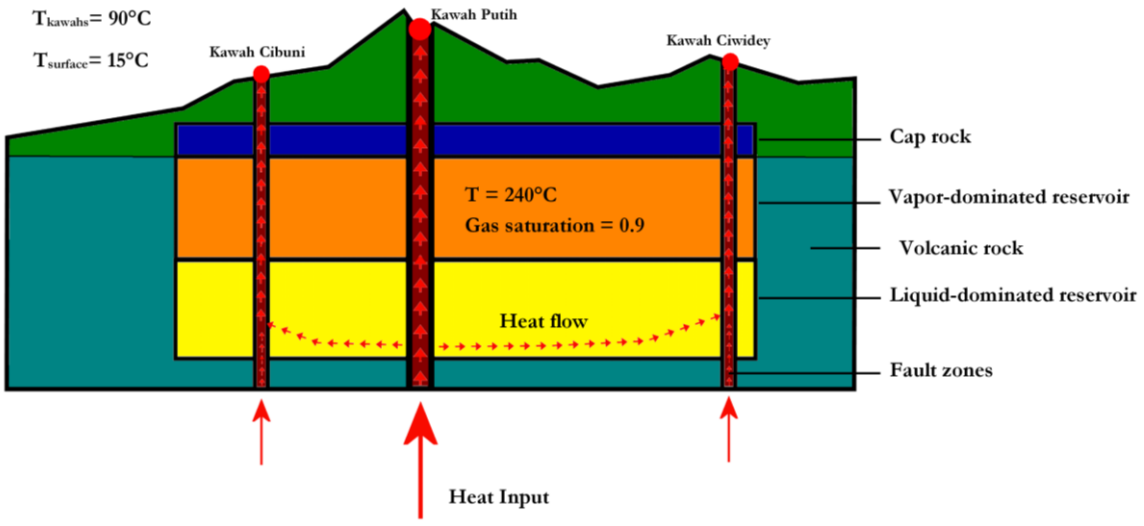

Figure 32 Simple conceptual model of the Patuha geothermal system

It is basically assumed that below Kawah Putih there is a large heat source. There is upflow of heat through the fault zones and lateral flow at depth of the reservoir rock. There are also minor upflow zones below the other surface manifestations, but based on the chemical composition of the waters, the assumption is made that the Kawah Putih source is the most important.

The flow of fluid is mainly concentrated in the reservoir and the fault zones. The permeability of these rocks is much lower than the surrounding volcanic rock and the cap rock.

9 Numerical model of the Patuha geothermal system

9.1 Introduction

Since modeling of a geothermal reservoir is rather complex, it is necessary to develop a simplified representation. There are several approaches to get to a good description of the dimensions, features and processes. For the dimensions, there are three options which all have their advantages and disadvantages. They are summed up below.

First option is a two-dimensional model. This is basically a vertical cross section of the reservoir (Figure 33). Important features, such as surface manifestations, faults and wells, can be extrapolated onto the line. The data points on or close to the cross section should be considered more accurate than the points which are extrapolated from a larger distance.

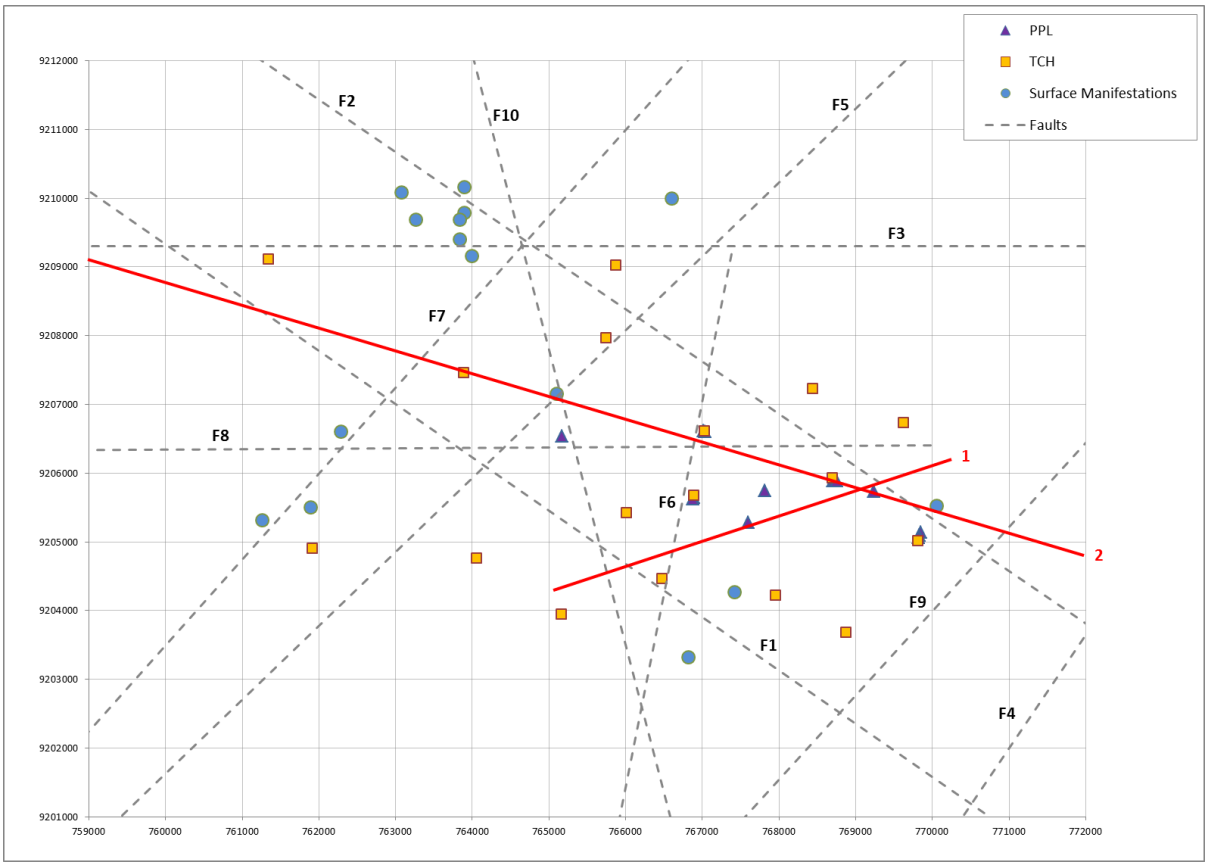

Figure 33 Example of two cross-sections that could be used for a two-dimensional model

Such a representation can give a good understanding of the processes in the reservoir. However, the model requires a value for all three dimensions (X, Y and Z), leading to the problem of the determination of the Y-axes. Since there are large uncertainties to this model type and its value to this thesis is limited, a two-dimensional model is not included.

This problem with the Y-axes can be solved by developing a radial symmetric model. The input of such a model only requires a value for the R (radial) and Z dimension. At a radial symmetric model it is assumed that there is a symmetrical arrangement of constituents around a central point. Within a circle all data can be represented on a line, the radius of the circle (Figure 34). This can work for point data (wells and surface manifestations), but will give problems for line data (for example faults). A simple example of such a model is presented in Paragraph 9.3.

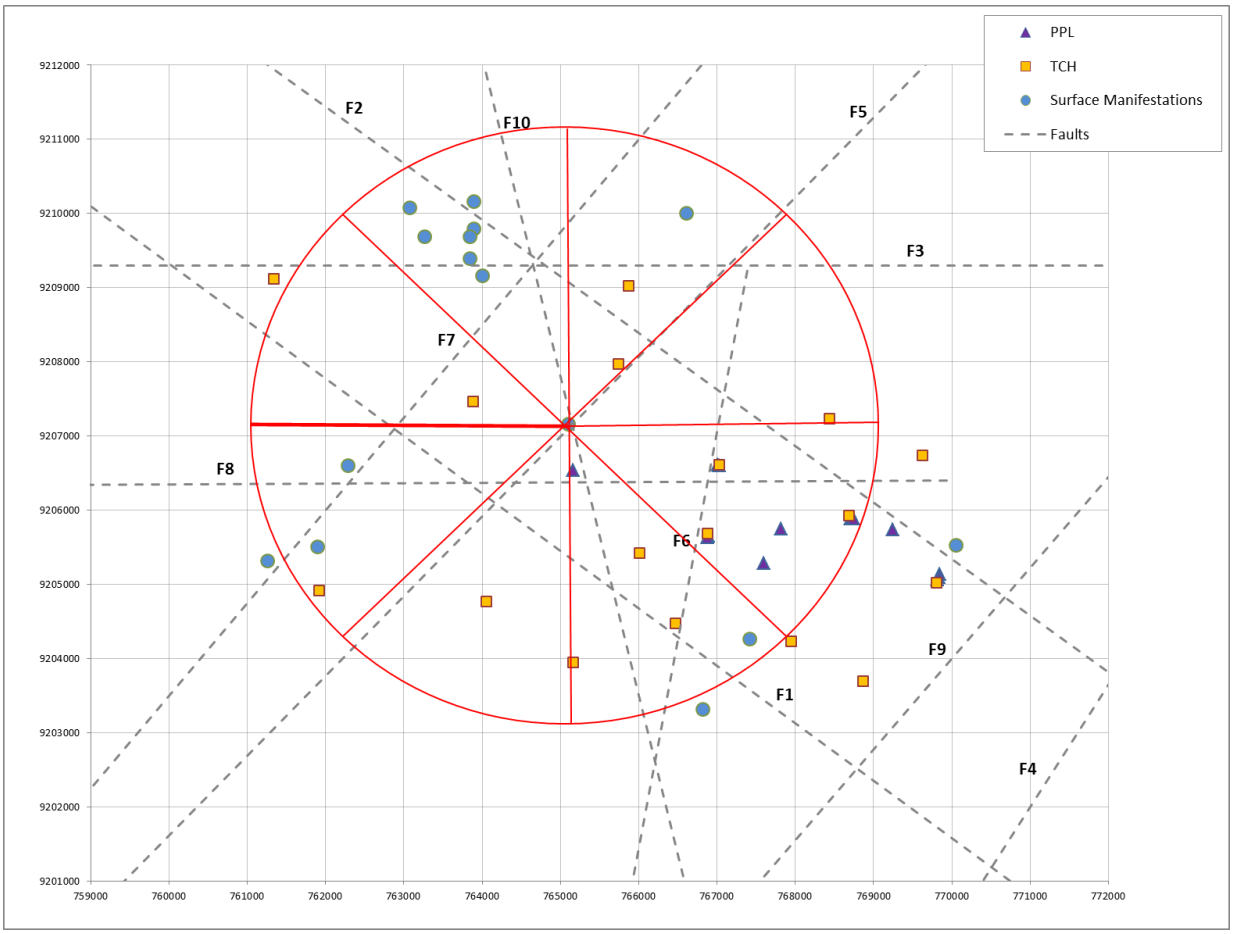

Figure 34 Example of a radial representation of the reservoir. The modeled area lies within the circle and the actual model is along radius.

The third option leads to the most representative model. The complications of the two-dimensional and the radial symmetric models do not hold for a three dimensional model. However, the addition of a third dimension results in a more complex model. The complexity of the model is mainly determined by the number of cells. The detail around the data point should be larger, resulting in smaller cells around these points. Furthermore, it is not possible to add multiple wells to one cell.

A three-dimensional model will give the best representation of the geothermal reservoir, but it is also the most complicated to develop. The two other model types can however add to the understanding and

visualization of the processes within the reservoir. Therefore a radial symmetric model will first be presented, followed by a simple three dimensional model.

9.2 Method

The software used to develop a numerical model for the Patuha vapor-dominated system is Petrasim, which is a graphical interface for the TOUGH2 family of simulators. The TOUGH codes have been developed by Lawrence Berkeley National Laboratory to simulate fluid flow and heat transfer in porous and fractured media.

TOUGH2 mainly solves mass and energy balance equations that describe fluid and heat flow in general multiphase, multicomponent systems. There is fluid advection, described by a multiphase extension of Darcy's law and diffusive mass transport in all phases. The flow of heat occurs by conduction and convection. The convective flow includes sensible and latent heat effects. Furthermore, there is the basic assumption that locally all phases are in thermodynamic equilibrium. Arbitrary nonlinear functions of the primary thermodynamic variables describe the fluid and formation parameters (Pruess, 1999).

Important in modeling vapor-dominated systems is the phase change that occurs. This can be done by using a set of variables that remain independent even as phase conditions change. A two-phase system can however also be directly created by switching from the use of basic thermodynamic variables (pressure, temperature) for single-phase conditions, to variables (saturation combined with pressure or temperature) when a phase change occurs (Pruess, 1999).

TOUGH2 requires a basic input to describe the flow system. This includes hydrologic parameters, constitutive relations of the permeable medium, thermophysical properties of the fluids, initial and boundary conditions and sinks and sources. Furthermore, TOUGH2 requires geometry data and time-stepping information. There is a selection of several EOS (Equation of State) modules. For the development of the model of the Patuha system, the first module is used, because it fits the best with the properties of the system. EOS1 provides a description of pure water as a liquid, vapor, and two-phase state. All water properties (density, specific enthalpy, viscosity, saturated vapor pressure) are calculated from the steam table equations as given by the International Formulation Committee (1967) (Pruess, 1999)

9.3 Radial symmetric model

9.3.1 Introduction

For a radial symmetric model it is important to take an area of the geothermal reservoir which shows little variation along the radius of the circle and remains representative for the several different features and data points in the area. Figure 36 Radial symmetric model. Color representation is given in Table 1shows the selected area with Kawah Putih as a central point extending approximately 4 kilometers to the hot

springs of Cimanggu and Baratunggul in the north, Cisaat in the west and Cibunggaok in the southeast. There are also several wells which fall into this range.

9.3.2 Assumptions

The radial symmetric model is developed to illustrate the basic flow mechanisms and temperature distribution of the Patuha vapor-dominated system. Due to the limitations of this type of modeling, the influence of the production and injection of fluids is not taken into account. Therefore the radial symmetric model is only used to describe the initial conditions and the steady-state situation.

Because of the limitations of the type of model (i.e. radial symmetric) and due to further simplifications, the modeling results will not be the same as the obtained data from the field, but it will give a simplified image of the studied area. A calibration procedure with the pressure and temperature data from wells has therefore not been carried out.

The measurements from surface manifestations are used as an input at the top of the model. Therefore two cells in the top layer are kept at a temperature of 90°C and 50°C, which are approximately the temperatures of respectively the crater lake of Kawah Putih and the hot springs of Rancawalini. The pressure of these cells is kept at the default setting, which is set at atmospheric pressure. At the bottom boundary of the model, the pressure and temperature are kept to 3.3 MPa and 240°C, coinciding with the maximum enthalpy of steam.

The other parameter which plays an important role in the flow within the model is the permeability. Since there are no direct measurements of the permeability, the values used by West JEC (2007) are used. These starting values are changed during the modeling process by trial & error. This results in the final permeability values, which are presented in the next paragraph.

9.3.3 Modeling input

Dimensions

The R-dimension of the model is based on Figure 34. The circle in the Figure includes all the necessary data points. The radius of this circle is approximately four kilometers. Therefore the size of the model in the R-direction will be 4000 meters. The depth of the model (Z-direction) is based on the pressure and temperature profiles and the conceptual model, which show that the vapor-dominated part of the system extends to approximately 500 m.a.s.l. (meters above sea level). The top is set at 2400 m, resulting in a total thickness of the model of 1900 m.

Layers

There are four different layers in the model (Figure 35). The top layer is an atmospheric layer with a thickness of 100 m ranging from 2400 m to 2300 m. This layer has no great relevance, but it is implemented to ensure vertical outflow from the reservoir. This layer is followed by a top layer of 700 m thick, ranging to 1600 m.a.s.l.. The third layer, between 1600 m and 1200 m, is the cap rock and the fourth

layer is representing the vapor-dominated reservoir. All the layers are divided into cells with a thickness of 100 m, except for the bottom layer. Here, an extra thin layer has been added at the bottom so that the influences of the boundary conditions on the system are minimalized. Thereby, the Z-divisions are set.

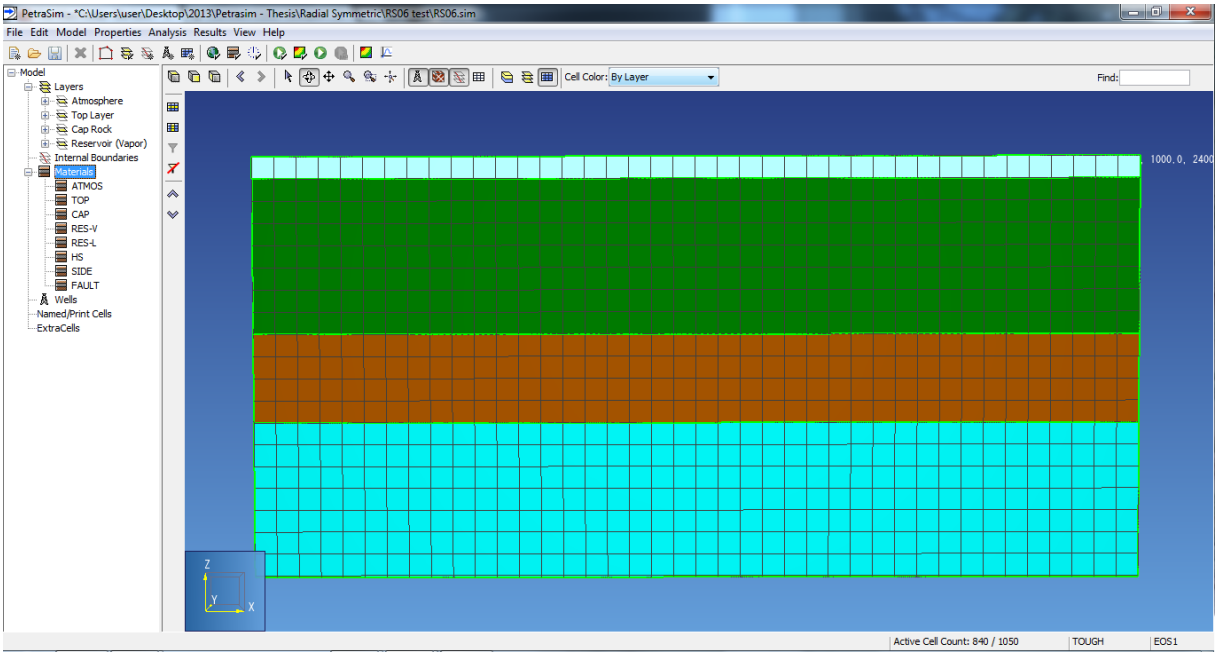

Figure 35 Layers of the radial symmetric model of the Patuha geothermal system. Atmospheric layer (white), Top Layer (green), Cap Rock (brown), Reservoir rock - vapor (blue).

Mesh

A radial mesh type is used. For the R-divisions a thickness of 100 m is chosen, what results in grid cells of 100 by 100 m. At both side boundaries, there is again a thin layer.

Material data

The materials are presented in Table 6. For the density, wet heat conductivity and specific heat of the different materials default settings were used. The values for these parameters are respectively 2600 kg/m^3, 1.8 W/m°C and 1000 J/kg°C. The porosity only deviates from the default settings (0.1) for the material representing the cap rock (0.01) and the side boundary (0.001), since at these layers the flow possibilities are limited or even assumed absent. For the material properties in this model, the permeability is the only important varying parameter. The values for the permeability assigned to the different materials are given in Table 6. The atmospheric layer is given a large value for the permeability, to ensure the flow towards this layer is without any restrictions

Table 6 Material properties of the radial symmetric model

Materials	Color	Description	XY Permeability [m²]	Z Permeability [m²]
ATMOS	White	Atmosphere	1.0	1.0
TOP	Green	Top layer	5.0E-16	5.0E-16
CAP	Purple	Cap rock	1.0E-18	1.0E-19
RES-V	Blue	Vapor-dominated reservoir	1.0E-13	1.0E-14
HS	Dark Red	Heat source	1.0E-13	1.0E-13
SIDE	Black	Side and bottom boundaries	0.0	0.0
FAULT	Dark Red	Fault (zone)	1.0E-13	1.0E-13

Figure 36 shows the radial symmetric model. The colors represent the materials which are assigned to the different cells. As can be seen the heat source is at the bottom left boundary in red. To prevent the heat source from depleting, the bottom (thin) layer has to be given a very large volume. There are also two corrections made by changing the permeability factor. The permeability of the top layer, above the left fault (in red), is increased by a factor 5 compared to the rest of the top layer in order to increase the flow to the surface. The permeability factor of the right fault on the other hand is set at 0.05, thereby decreasing the flow by a factor 20 compared to the left fault.

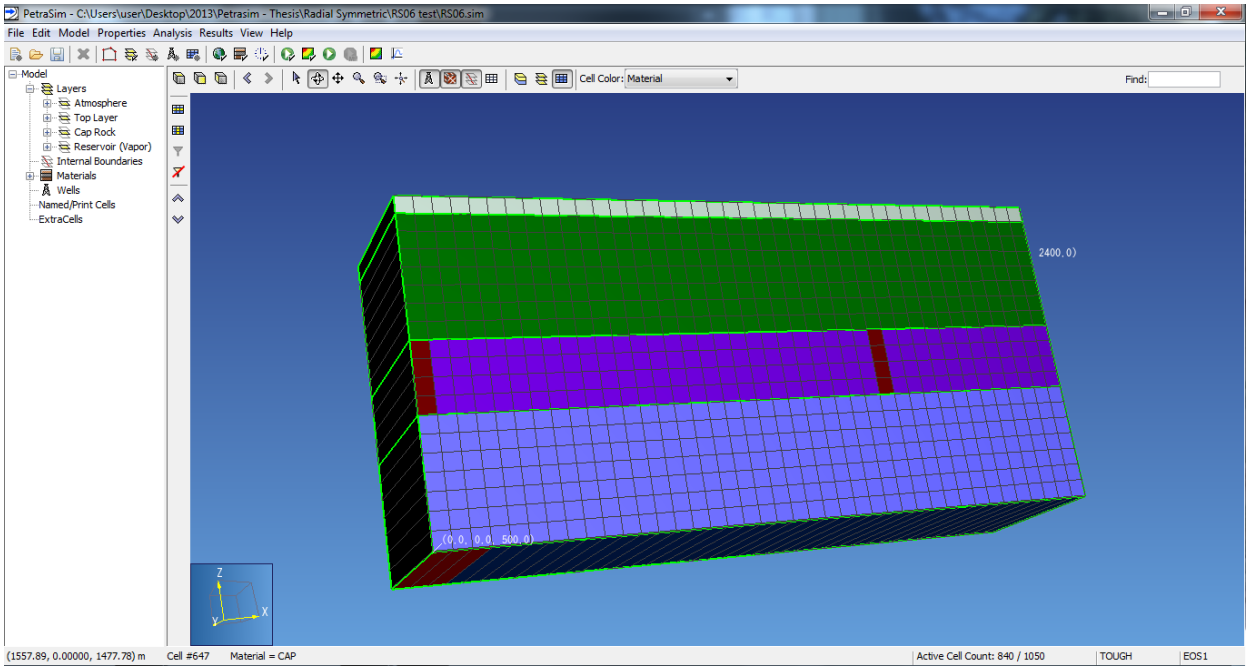

Figure 36 Radial symmetric model. Color representation is given in Table 1

9.3.4 Results

The results for this model are presented by a temperature distribution in Figure 37 to Figure 39. The large temperature difference between the bottom (thin) layer and the rest of the model, results in an upward heat flux. Since the permeability of the heat source is much larger than the rest of the bottom layer, most of the heat flux towards the surface is generated by the 3 cells representing this heat source.

The same accounts for the two faults, which have a large permeability compared to the cap rock. It can therefore be seen that the heat flow to the surface is mainly through these two faults. At the end of the used time frame, the temperatures of the top layer approximately reach the fixed temperature of both the surface manifestations. It can also be seen that after this same time frame, the layer representing the vapor-dominated reservoir, has an overall temperature of 240°C.

Overall, the model can be described as a large uniform vapor-dominated reservoir, which is sealed by a low permeability cap-rock. This can be compared to the model I by Ingebritsen and Sorey (1988), as described in Paragraph 2.4.

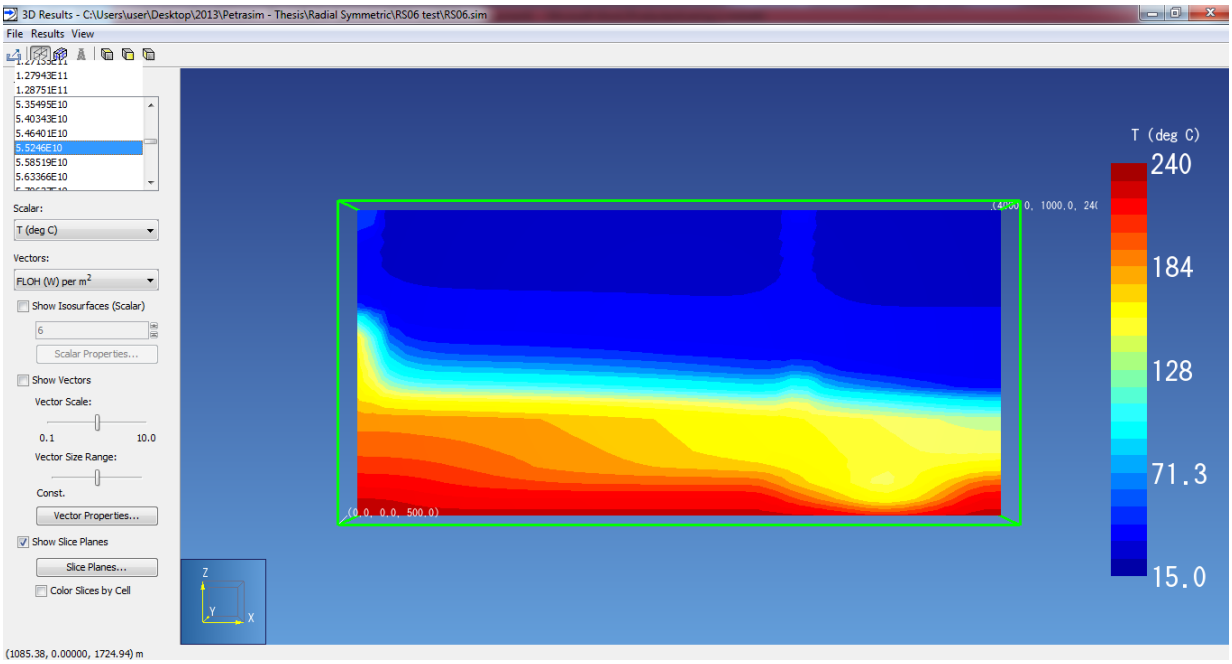

Figure 37 Temperature distribution of the radial symmetric model at t=5.5246E10 sec

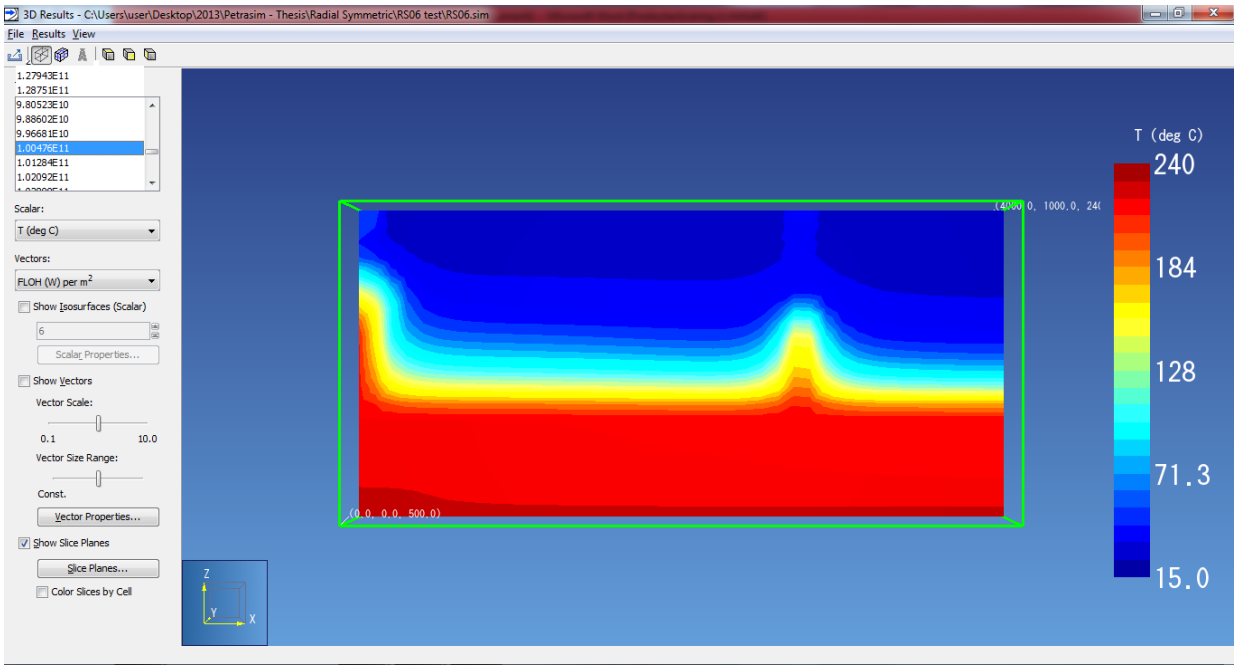

Figure 38 Temperature distribution of the radial symmetric model at t=1.00476E11 sec

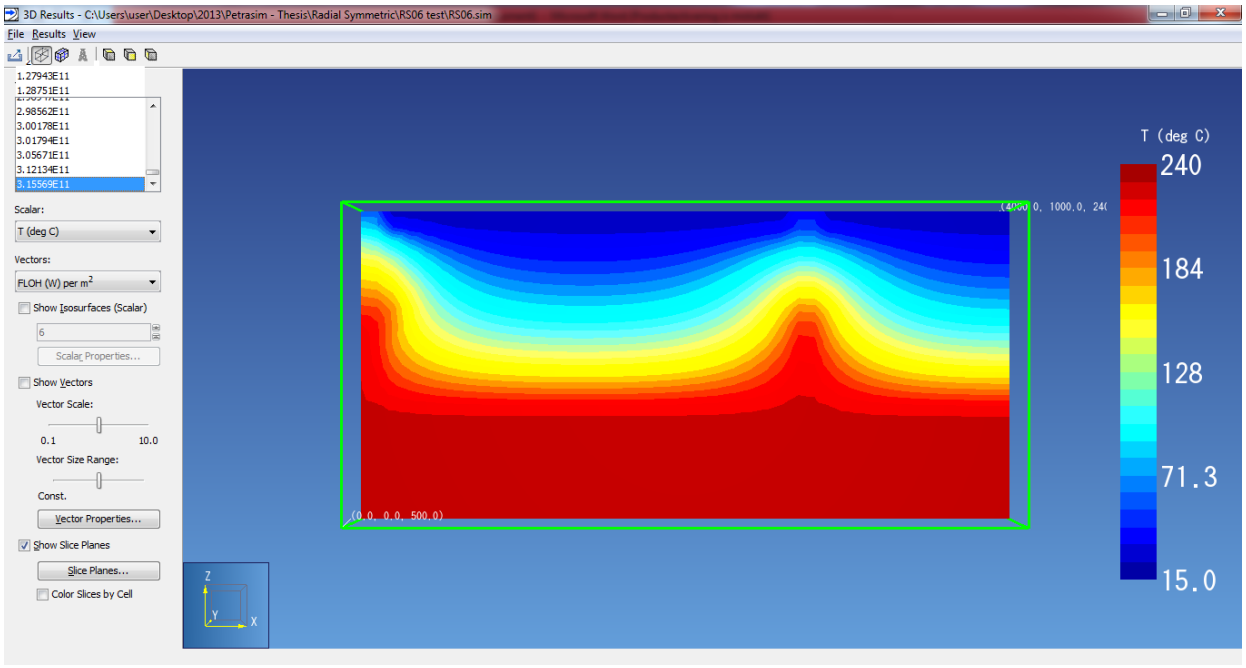

Figure 39 Temperature distribution of the radial symmetric model at t=3.15569E11 sec

9.4 Three dimensional model

9.4.1 Introduction

A three dimensional model is developed based on the conceptual model presented in Paragraph 8.4. The model is used to give a representation of the natural state situation of the Patuha vapor-dominated reservoir. The pressure and temperature conditions of the vapor-dominated reservoir in the model are given the theoretical value for the maximum enthalpy of steam (Paragraph 2.3). After this a comparison between the pressure and temperature data from the field and the model output is presented to obtain insight in the anomaly between the two.

For the developing process, a combination of (1) theoretical knowledge (Paragraph 2.3 to 2.5), (2) data obtained from the field (presented in Chapter 4 to 7), and (3) parameters obtained by trial and error is implemented in the model. Only full-sized wells are used to compare the model output with the field data.

9.4.2 Assumptions

Since the model size will in the end determine a large part of the runtime it is important to keep the model area as small as possible, while still producing reliable results. Figure 40 shows the concession area of the Patuha reservoir (by Geo Dipa Energi) and the selected area which is represented by the model. As can be seen, all the important surface manifestations lie within the model area. Since these are an indication for up- and outflow zones of the geothermal reservoir, it is important to include these all in de model.

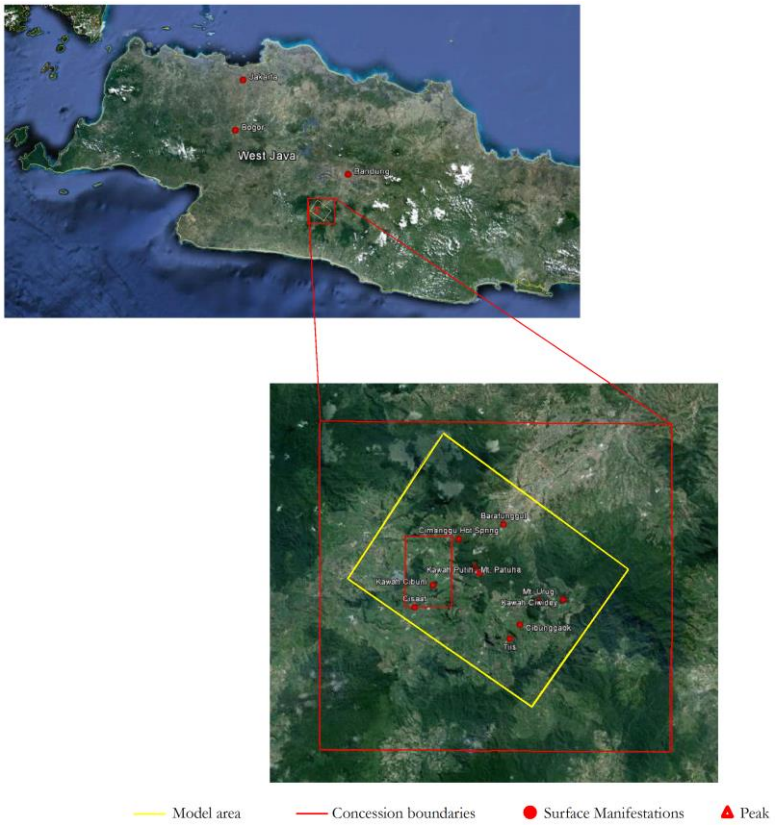

Figure 40 Concession area of Geo Dipa Energi and the model area

As can be seen in Figure 41, the model area is in line with the main fault structures and is therefore rotated by an angle of approximately 34°. All of the important surface manifestations and wells, as well as the expected boundaries of the steam cap, are falling within the model area.

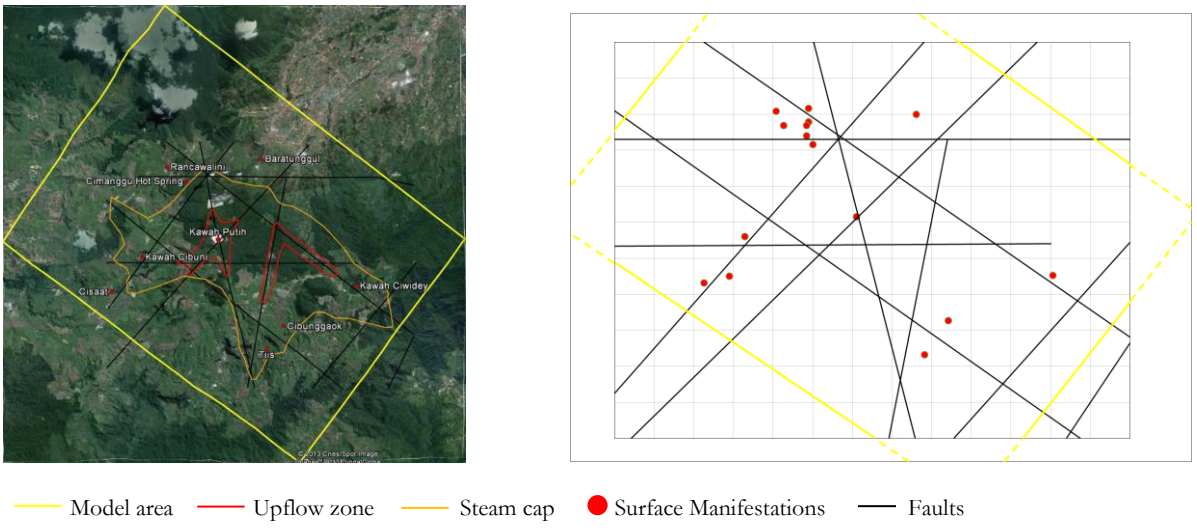

Figure 41 Model area and main faults and steam cap boundaries as interpreted by West JEC (2007)

As stated in Paragraph 2.3, the maximum temperature and pressure of the fluids in a vapor-dominated reservoir is approximately 240°C and 3.3 MPa. To make a comparison between the measured well data and the theoretical value, the cells that represent the vapor-dominated system will be kept at the mentioned conditions.

Data on the surface manifestations shows us that the temperatures of the kawahs (Ciwidey, Cibuni and Putih) are approximately 90°C. The atmospheric temperature in the area is approximately 15°C on average. The pressure at the surface is atmospheric (~0.1 MPa) over the whole model. West JEC has also given an interpretation of the size of the steam cap and the upflow zones (Figure 29 and Figure 41). This interpretation is used to set the boundaries of the reservoir in the model. Other important parameters of the modeling process are the permeability and the flow of heat entering the model. Both parameters are determined by trial and error.

9.4.3 Modeling input

Dimensions

The final model is cut from a rectangle of 16.74 kilometers in the X-dimension and 16.44 km in the Y-dimension. The cropped part is 13.44 km in the northwest direction and 10.34 km in the southeast direction (Figure 42). To include the total range of all the wells, the depth of the model is set at -500 m.a.s.l.. The top is varying between 2424 and 1044 m.a.s.l.. Since there is a varying elevation of the top layer, there is no atmospheric layer in the three dimensional model.

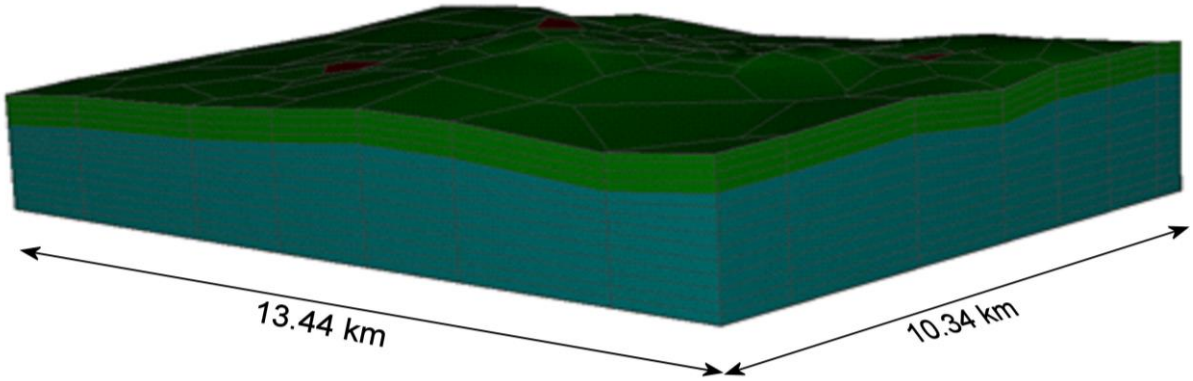

Figure 42 Dimensions of the final model

Layers

There are seven different horizontal layers defined in the model, each subdivided in a number of cells (Figure 43). The top and bottom layer are both thin layers with a thickness of only 10 m. The addition of these two thin layers at the upper and lower boundary of the model limits the effect of any boundary conditions which are added to these layers.

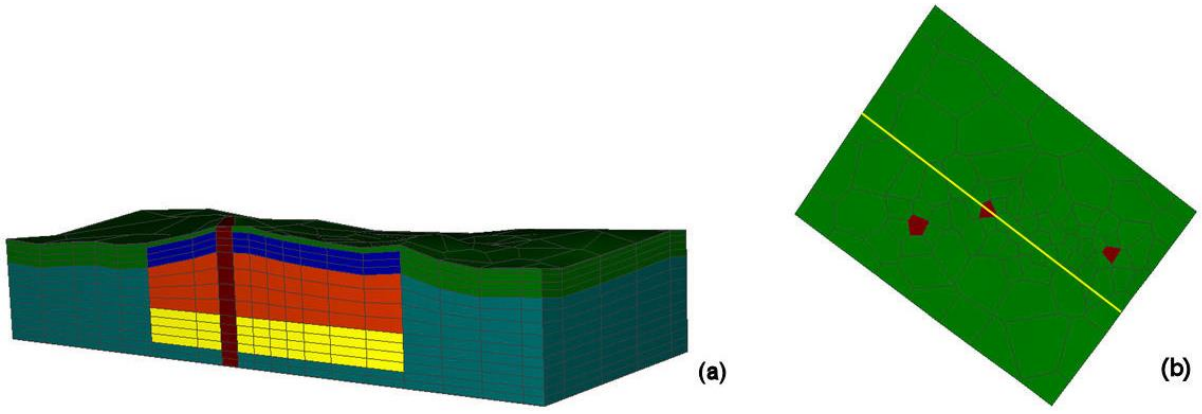

Figure 43 (a) Cross section of the final model (b) Location of the cross section. The red dots are the surface manifestations at Cibuni, Ciwidey and Kawah Putih

To insert topography into the model, digital elevation data (DEM) provided by USGS and NASA (2000) is used. The DEM data is converted to a xyz-file, which can be uploaded in Petrasim as a top layer. This xyz-file is also used for the top of the second top layer, the top of the cap rock and the top of the vapor-dominated reservoir, by subtracting the thickness of these layers from the elevation at the different coordinates.

Table 7 Layer input

	Top (m)	Base (m)	Thickness (m)	Number of cells (in vertical direction)
Top Layer 1	-	-	10	1
Top Layer 2	-	-	90	1
Cap Rock	-	-	400	3
Vapor-Dominated Reservoir	-	500	Variable	4
Liquid-Dominated Reservoir	500	-200	700	4
Bottom Layer 1	-200	-490	290	2
Bottom Layer 2	-490	-500	10	1

Mesh

Both a regular and a polygonal mesh are used as input for the model. At a polygonal mesh, the cell size near wells can be reduced with respect to the other cell sizes. Therefore the data retrieved from the model shows a higher resolution. Furthermore, the distance between wells in the model can be smaller because the cell size can be decreased locally. The overall maximum mesh area is $4.0*10^6$ m². The maximum area near the cells is $3.0*10^5$ m². This results in a number of cells of 660.

Material data

The different substrate rock types are presented in Table 8. Similar to the radial symmetric model, default settings are used for the density, wet heat conductivity and specific heat of the different materials. The values for these parameters are respectively 2600 kg/m³, 1.8 W/m°C and 1000 J/kg°C. For the three-dimensional model, the porosity is also kept at the default setting of 0.1. The permeability is also at this model type the most important variable for the material properties. The different materials and the corresponding horizontal and vertical permeabilities are presented in Table 8 Material properties of the three-dimensional model

Table 8 Material properties of the three-dimensional model

Abbreviation	Color	Description	XY Permeability [m²]	Z Permeability [m²]
QVR	Green	Quaternary volcanic rock	5.0E-17	5.0E-18
TVR	Greenish-blue	Tertiary volcanic rock	1.0E-17	1.0E-17
CAP	Blue	Cap rock	1.0E-17	1.0E-18
RES-V	Orange	Vapor-dominated reservoir	1.0E-13	1.0E-14
RES-L	Yellow	Liquid-dominated reservoir	5.0E-14	1.0E-14
FAULT	Dark Red	Fault (zone)	5.0E-14	2.0E-14
HS	Red	Heat source	1.0E-13	1.0E-13

The materials are ascribed to the different layers (Figure 44 to Figure 48). The Quaternary volcanic rock reaches a depth of the top of the vapor-dominated reservoir. Below this layer, the material is considered to be Tertiary volcanic rock. The reservoir in total includes the cap rock, vapor-dominated reservoir and the liquid-dominated reservoir. These material types can be considered as volcanic rock which is altered by either fracturing or argillic alteration, resulting in different permeabilities. The material type FAULT is included to ensure sufficient throughflow at specific locations from the bottom to the top of the model. Therefore this material type is given to the cells which are below the main surface manifestations (kawah Putih, kawah Ciwidey and kawah Cibuni). These three locations will function as an upflow zone due to the relative low permeability of the FAULT material. The HS rock type is only applied to the cell of the bottom layer which lies beneath kawah Putih, mainly to clarify that this cell is the main heat source and therefore upflow of heat will take place from this cell.

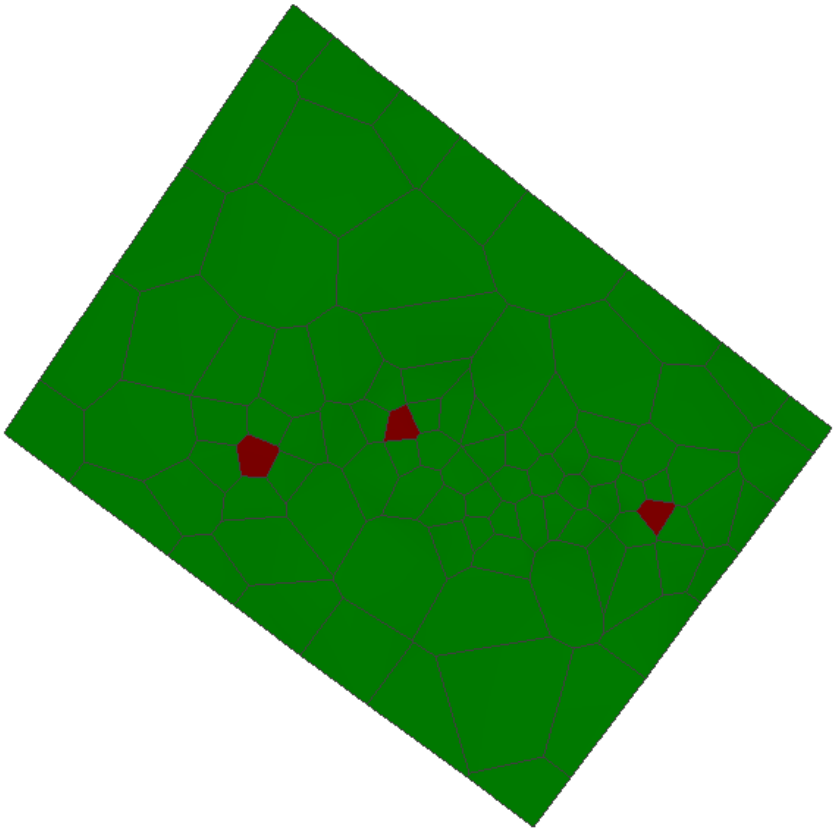

Figure 44 Horizontal cross section of the top layer

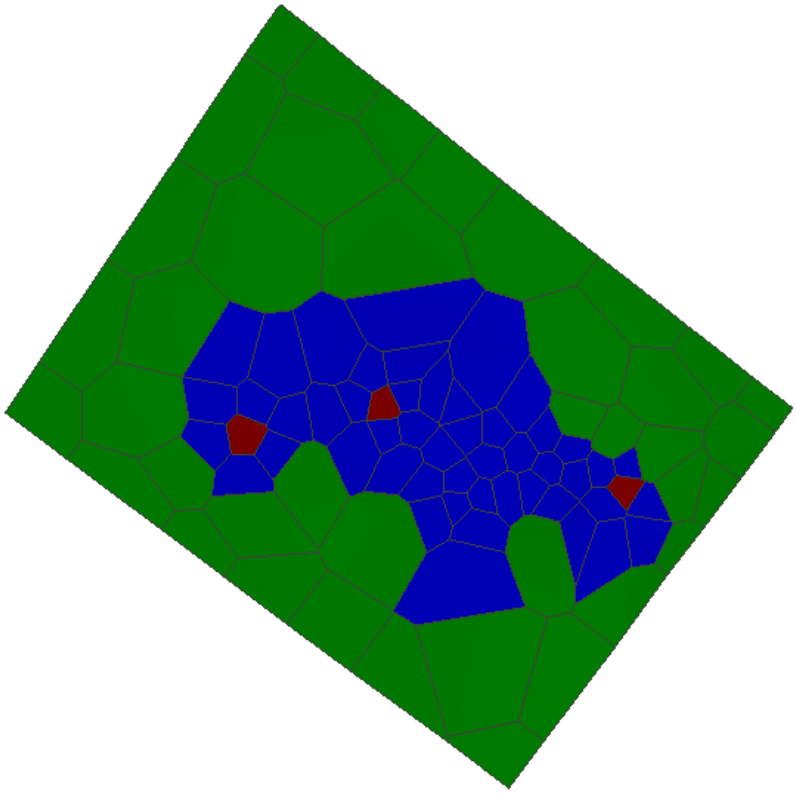

Figure 45 Horizontal cross section of the cap rock layer

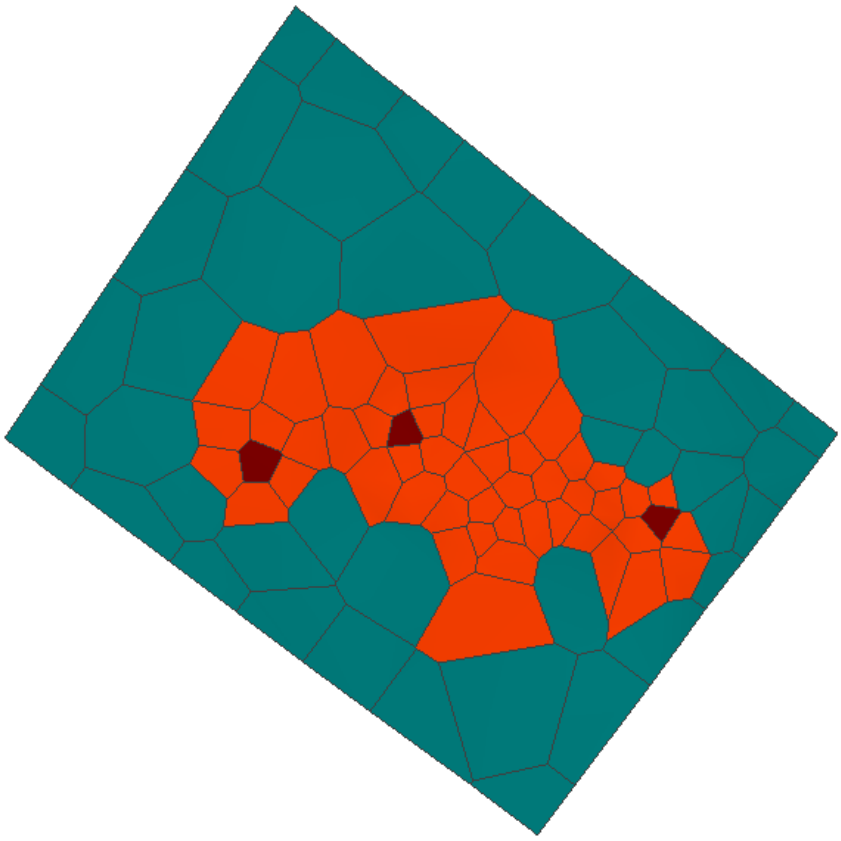

Figure 46 Horizontal cross section of the vapor-dominated reservoir layer

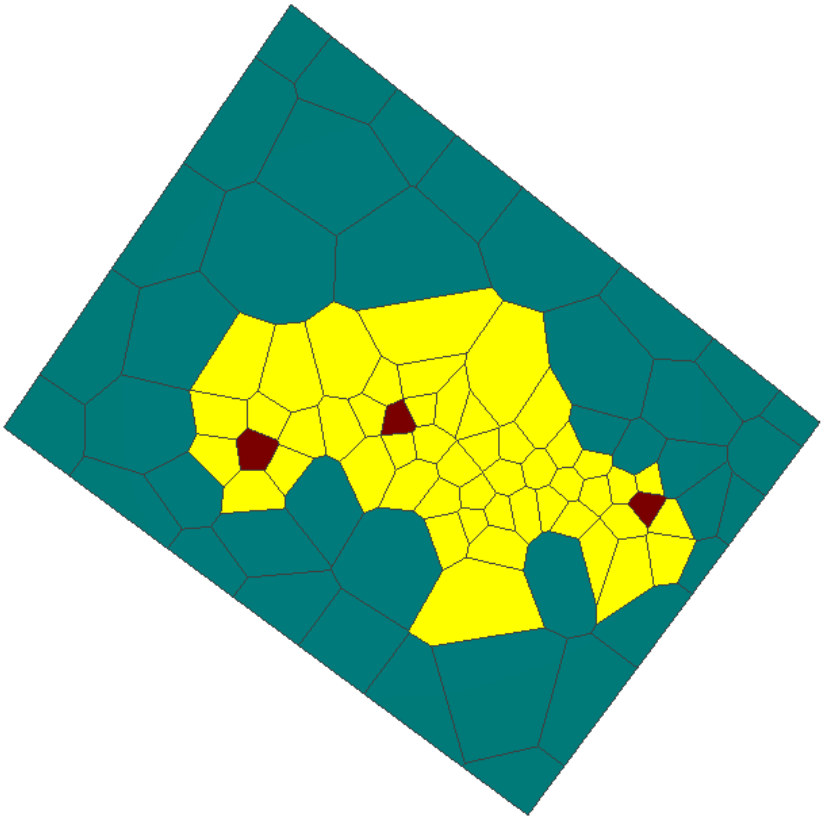

Figure 47 Horizontal cross section of the liquid-dominated reservoir layer

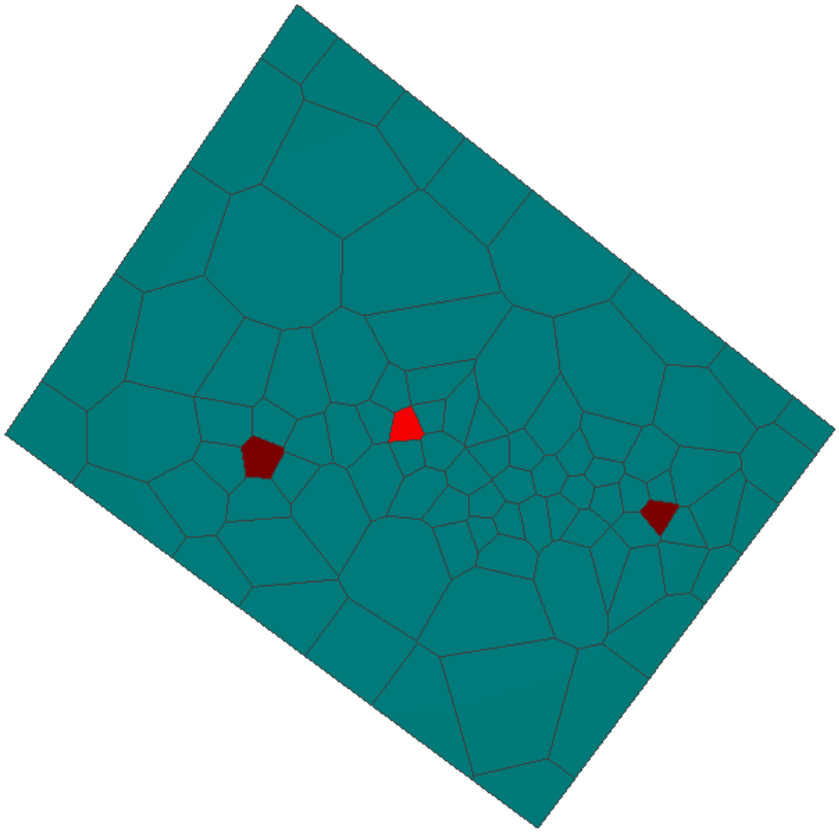

Figure 48 Horizontal cross section of the bottom layer

Initial conditions

Initial conditions can be ascribed to layers or to individual cells. As mentioned, thermodynamical conditions are set to a fixed state for the vapor-dominated reservoir. The temperature of these cells is 240°C and since steam it is expected to be dominantly present for this layer, the gas saturation is set at 0.9 (Figure 49). This parameter is not set at 1 (only gas-phase), since there is always liquid present in the interstitial pores (Paragraph 2.3). The top and bottom layer are also given a fixed temperature and pressure or gas saturation.

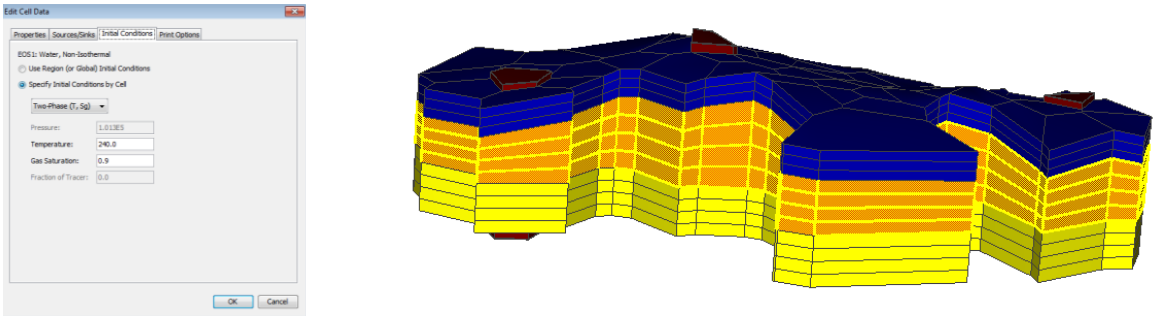

Figure 49 Initial conditions for the vapor-dominated reservoir

The temperature of the top layer is set at 15°C with exception of the cells which represent kawah Putih, kawah Ciwidey and kawah Cibuni. These cells have a fixed temperature of 90°C. The pressure of the top layer is uniformly set at $1.013*10^5$ Pa, which corresponds with atmospheric pressure. The temperature of the bottom layer is set at 250°C, with exception of the cells below the three kawahs. The temperature of these cells is respectively 280°C for kawah Ciwidey and kawah Cibuni and 300°C for kawah Putih, since the latter is acting as the main heat source.

At the bottom layer a certain flow of heat is added to the model. These values are obtained by trial and error. With exception of the cells below the kawahs, this flow is $1*10^4$ J/s. The heat input below kawah Ciwidey and kawah Cibuni is $1*10^5$ J/s and the input below kawah Putih is $1*10^6$ J/s. To make sure that the heat flow from the cells of the bottom layer will remain constant over time and will not deplete, these cells are given a larger volume.

9.4.4 Results

Temperature distribution

The model is run for a sufficient time period to reach stationary conditions. Figure 50 shows the temperature distribution at the end time. The temperature at the vapor-dominated reservoir is fixed at 240°C, represented by orange. This results in a large temperature increase over a small depth range. Around the location of kawah Putih the heat source is clearly visible in dark red.

The temperature at the boundary of the model is much lower, showing a more gradual temperature gradient. This is as expected since there is little flow of fluid through the low permeable volcanic rock.

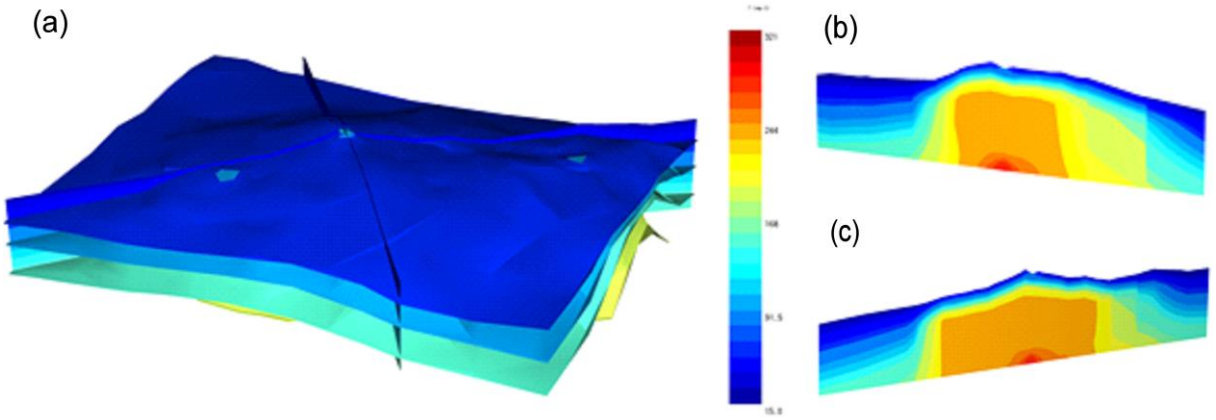

Figure 50 Temperature distribution. (a) shows the location of the cross section with kawah Putih at the cross point, (b) shows the cross section in the X-direction and (c) shows the cross section in the Y-direction.

The temperature profiles which are obtained from the wells are also compared with the output of the model. The results are presented in Figure 51. There are several wells from the model show a similar pattern as the measured profiles, especially the wells at location A, H, and U. The measured temperature is lower for all the wells. The temperature difference between the field measurements and the theoretical value generally lies between about 20°C and 60°C, with a few outliers to about 80°C. The temperature at these locations should be decreased with about 20 to 60 degrees to obtain an acceptable match with the two data sets.

The modeled temperature profiles of wells at location D deviate more from the measured field data. Although field measurement show the expected trend, with a large increase of temperature at the depth followed by a close to constant temperature over a certain depth range, probably representing the cap rock and the vapor-dominated reservoir, the gap between the profiles obtained from the model and those from the field data is much larger than at the locations mentioned above (>100°C). However temperatures at larger depths (corresponding with the vapor-dominated reservoir), the gap decreases to about 20°C.

The offset between the two profiles could be explained by a difference in the depth and/or thickness of the cap rock. When depth of the cap rock layer in the model is decreased by about 200 meters and the temperature will be decreased by about 20°C, the profiles obtained from the model will show a better match to the field data.

The temperature profiles at location G, V, W and Z do not show any resemblance between the measured and modeled data. The field data at these locations deviates substantially from the temperature profiles.

At location G, the field data shows a constant temperature gradient with depth. For Well 01, the temperature is almost constant with depth and Well 02 has a constant gradient of approximately 14°C per 100 meters.

The well at location W shows a constant temperature over a large depth range (from the top of the well to approximately 900 m.a.s.l.). At lower depth the temperature increases with a similar pattern to that of the modeled temperature, only with an offset of about 50°C.

At location Z, the well only reaches a depth of 1237 meters. From the top of the well until this depth, the temperature gradient is approximately constant at 5°C per 100 meters.

The field data at location V has a constant small gradient until about 1100 m.a.s.l.. With the exception the peak in temperature around 600 m.a.s.l., there is a larger close to constant temperature gradient of approximately 11°C per 100 meters at larger depth. Due to the particular temperature profile at this location, the field data can probably not be matched with the model data.

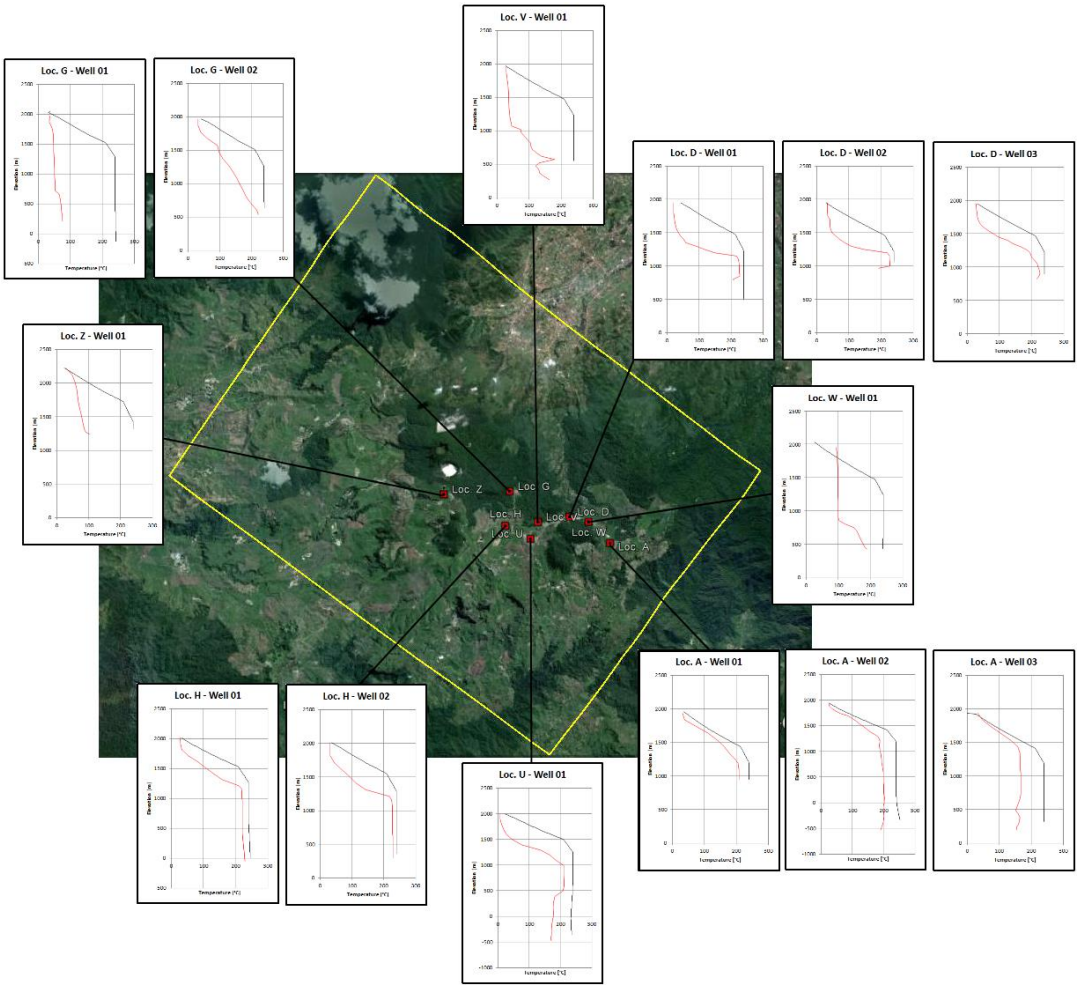

Figure 51 Temperature profiles of the wells. The red line corresponds with the measured temperature. The black line corresponds with the temperature obtained from the model.

Pressure distribution

The main focus at the modeling process was on the temperature distribution. Besides from the atmospheric pressure conditions, no cells or layers are applied with a fixed pressure. There is however a fixed gas saturation factor applied for several layers. This results in the pressure distribution presented in Figure 52. As can be seen in Figure 52 (a) and (b), there is a gradual gradient at the boundaries of the model. At the location of the reservoir, the pressure distribution deviates from this gradient. Over the depth range of the vapor-dominated reservoir, the pressure is close to constant. Furthermore, the pressures are lower than outside the modeled reservoir.

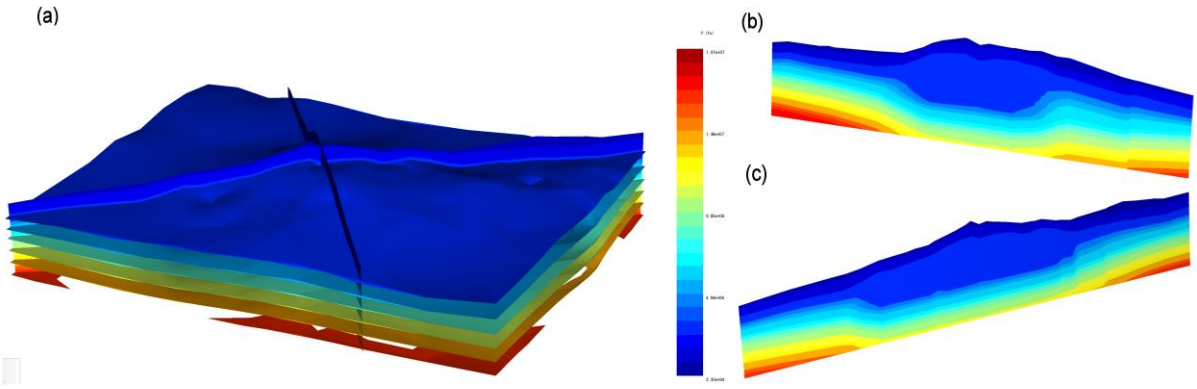

Figure 52 Pressure distribution. (a) shows the location of the cross section with kawah Putih at the cross point, (b) shows the cross section in the X-direction and (c) shows the cross section in the Y-direction.

The pressure profiles obtained from the field data and the model are presented in Figure 53. Only for the well at Location Z there is no field data available.

There are seven wells that show a similar pressure profile for the field data and the model, namely Well 02 and 03 at Location A, Well 01 and 02 at Location G, Well 01 at Location H, and the wells at Location U, V and W. Although the pattern of the profile is the same, the offset is substantial. The offset of the pressure diverses between 0.9 MPa and 3.4 MPa and for the elevation between -340 m and +700 m. Also, the field data suggests a constant pressure over a certain depth range, including the top layer, the cap rock and the vapor-dominated reservoir. As can be seen in the profiles obtained from the model, the pressure is constant within the vapor-dominated reservoir, but decreases gradually to the surface.

For the other wells, the pattern is not as distinct as for the wells mentioned above. This is mainly because the data obtained from the field only show a close to constant pressure over depth. Therefore the pressure data from the model is difficult to compare to the field data. It is possible that these wells do not reach a sufficient depth and therefore only show the constant pressure corresponding to the upper layers (top layer, cap rock and reservoir rock).

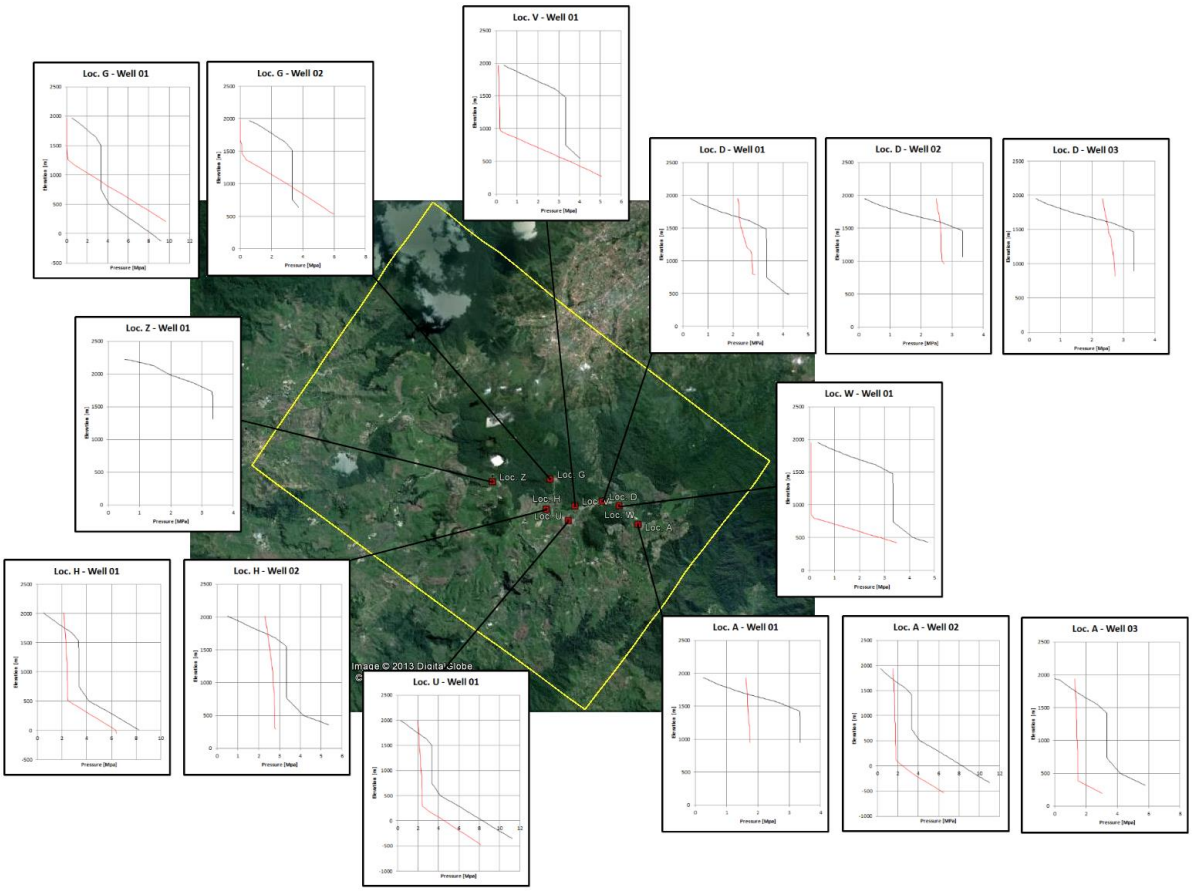

Figure 53 Pressure profiles of the wells. The red line corresponds with the measured temperature. The black line corresponds with the temperature obtained from the model.

Correction factor

For the wells that show a similar pattern between the field data and the model data, an attempt has been made to match data sets by shifting the temperature and pressure profiles obtained from the model by a certain temperature or pressure and elevation. The result is presented in Figure 54. The corrections can be applied to the model, thereby resulting in a natural state model which closely resembles steady-state situation of the Patuha vapor-dominated reservoir.

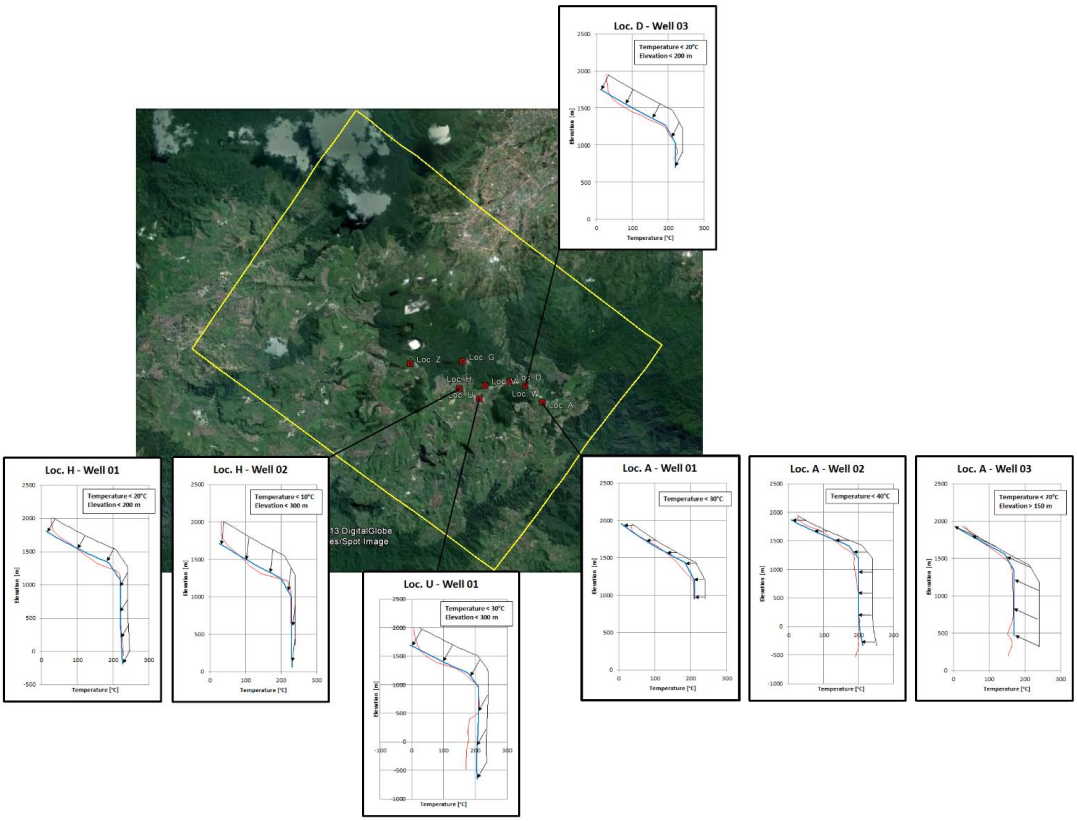

Figure 54 Manually corrected temperature profiles of the wells that originally show a similar pattern as the field data.

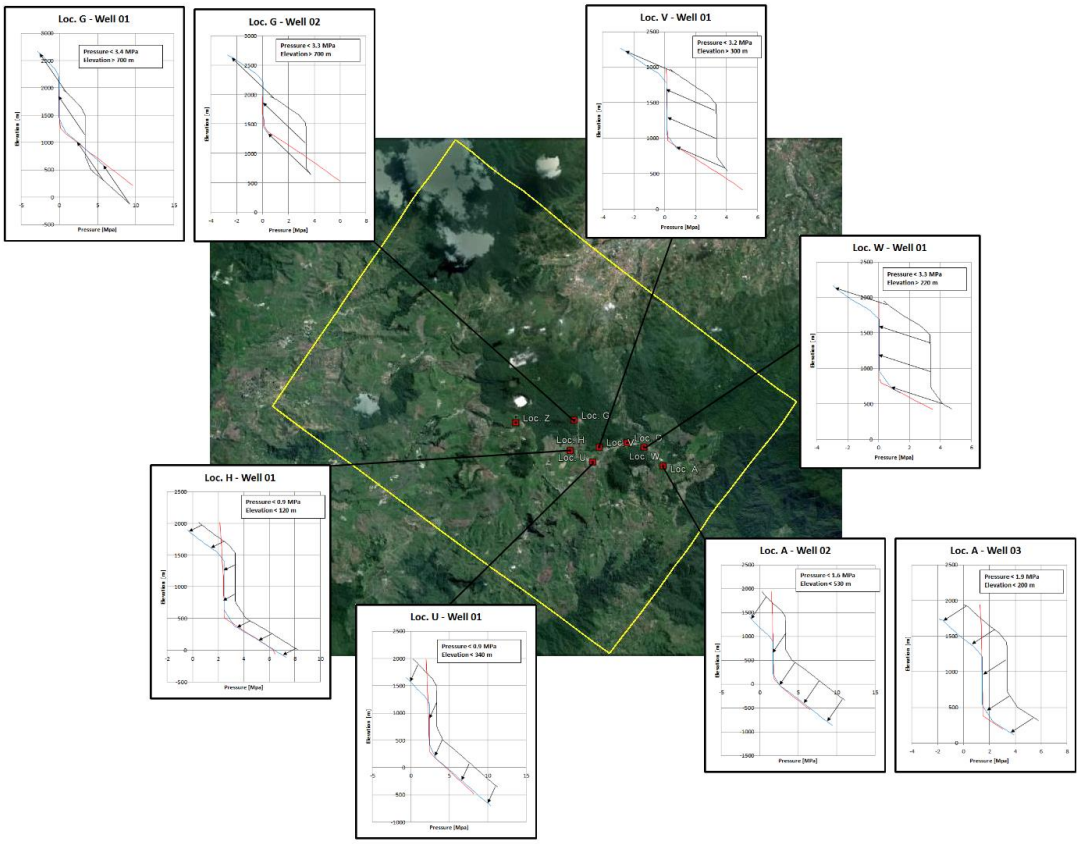

Figure 55 Manually corrected pressure profiles of the wells that originally show a similar pattern as the field data.

Calibration

In an attempt to obtain a better match with the well data, several modeling parameters are adjusted. The main focus is on the properties of the vapor-dominated reservoir (RES-V). For the calibration process, the permeability and the initial conditions (temperature) are the parameters that are adjusted. As described in the previous Paragraph, the elevation of the different layers also differs from the well data. This is illustrated by the deviation along the Y-axis in Figure 54 and Figure 55. Since the adjustment of the elevation of the layers is a complicated and time-consuming matching process, it has not been carried out in this study.

As described in Paragraph 9.3 at the modeling input, the temperature of the vapor-dominated reservoir is kept fixed at 240°C. This temperature has not been measured in any of the wells. The wells that show a similar pattern (Figure 54 Manually corrected temperature profiles of the wells that originally show a similar pattern as the field data. all show lower temperatures, varying between 170°C and 230°C. Since the vapor-dominated layer is assumed to be homogeneous in the model, the initial temperature conditions should also be the same for all the cells. It is possible to lower the initial temperature of the vapor-dominated reservoir by the most common deviation of 20°C. The result of this adjustment will however give a similar output, only with a displacement of 20°C. This will give a better match for the few wells that actually have this deviation, but will not be of much value for the other wells. Therefore this adjustment is not presented in this study.

Another option is to adjust the permeability of the vapor-dominated reservoir or the fault zones. This will result in a higher flow rate through the reservoir, but since the temperature conditions for vapor-dominated layer are fixed this will not influence the pressure and temperature output of the model. Therefore this has adjustment is not applied to the model.

A third option is to let go of the fixed initial conditions of the vapor-dominated reservoir. The pressure and temperature conditions representing the ideal conditions for a vapor-dominated reservoir structurally give to high estimations, as illustrated by Figure 54 and Figure 55. When the initial conditions will no longer be fixed, the temperature and pressure of the reservoir will slowly decrease. When the model is then run for a certain time, the temperature and pressure in several wells shows a better match than before.

For the temperature, a selection of the result is presented in Figure 56. The wells at location A and H show a better match with the field data, although there is still an offset along the Y-axis. For the wells at locations D, G and U, there is still a substantial difference in temperature distribution. However, the new model better resembles the temperature profiles obtained from field data than the original model.

Figure 57 shows a selection of the results for the pressure distribution. As can be seen, the new model gives a better pressure distribution in several wells, especially those at location A, location U and well 01 at location H. For other wells (Loc. G, Loc. V and Loc. D) the pressure distribution in the model still deviates substantially from the well data. For location D and well 02 at location H the model even gives a large underestimation of the pressure.

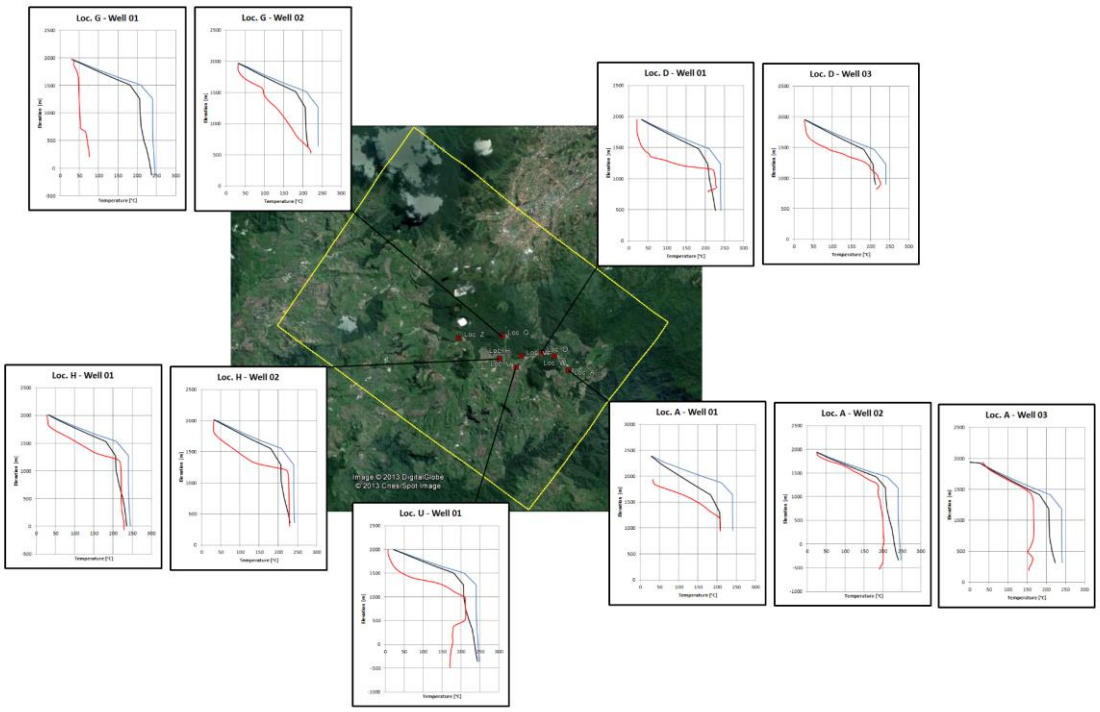

Figure 56 Temperature distribution. The red line represents the field data, the black line shows the output of the renewed model and the blue line gives the output from the original model.

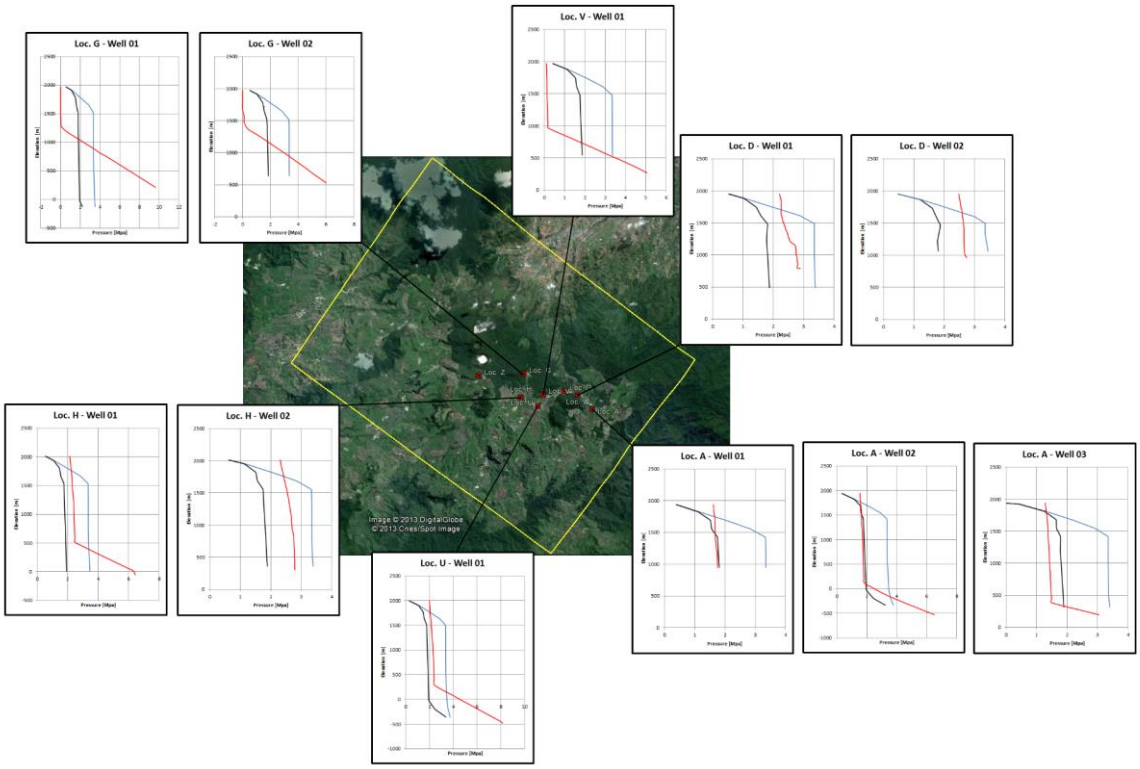

Figure 57 Pressure distribution. The red line represents the field data, the black line shows the output of the renewed model and the blue line gives the output from the original model.

10 Discussion

For several point measurements, the output of the model shows a similar pattern for the pressure and temperature profiles as the field data. These findings show that at least part of the Patuha system resembles the theoretical design of a vapor-dominated geothermal reservoir. This implicates that the use of a simple straightforward reservoir model based on the theoretical design can be sufficient for simulating the natural state of the Patuha system. By including small adjustments to the theoretical parameters, the reservoir model can ben calibrated to the field data. The numerical model that results from this calibration process can be used to give an estimation of the size of the resource and can even be used to design a development plan.

The simplicity of the model design has several advantages over a more complex approach, like the model developed by West JEC (2007). The presented model mainly consists of three homogeneous segments, the cap rock and the (vapor- and liquid-dominated) reservoir rock. These are surrounded by volcanic rock and only crosscut by a few fault zones. The assumption of homogeneity may not give an accurate representation of the subsurface, but the results show that the field data can be approximated. The West JEC-model of the Patuha system also shows a reservoir surrounded by homogeneous volcanic rock. The reservoir itself however, shows a large variety in material properties (with permeability as main variable) assigned to cells. There is no direct data from the field that indicates such large differences in petrology. The model by West JEC implicates a high accuracy by the complex approach, but this method palliates a large uncertainty factor on the reservoir properties. Moreover, the development and calibration of this model is more complicated and time consuming than the more simple and straightforward approach that is presented here.

Despite the several pressure and temperature profiles that show a similar pattern to those obtained from the field, there are also points in the model that do not resemble the well data. These profiles from the model are therefore difficult to accurately match with the field data. This shows that the homogeneity of the different reservoir layers cannot be applied to the whole area. It might be necessary to add a certain lateral variation in petrological parameters, so that the reservoir area is divided into a few segments with different permeabilities. Furthermore, it has to be stated that the method of shifting the pressure and temperature profiles obtained from the reservoir model with a certain elevation and pressure or temperature is not irrefutable. However, it helps to illustrate the gap between the output of the model and the field data.

When the initial conditions of the vapor-dominated reservoir are no longer fixed, the model shows an improvement compared to the original model. However, since the vapor-dominated reservoir is assumed to be homogeneous, it is not possible to obtain a good match for all the wells. The differences between the pressure and temperature profiles obtained from the wells are large for this. The renewed model however gives a good match for several wells and shows a better output for most of the other wells. When a better match between the field data is required, the assumption of homogeneity can no longer hold.

11 Conclusion

The analysis of the field data shows that the Patuha vapor-dominated reservoir is a geothermal resource which holds great potential. It can therefore be of substantial value to the Indonesian government in order to increase the percentage of geothermal energy on the total energy supply. Since the production of the Patuha reservoir has not yet been initiated, the development of a numerical model of the area has a high priority.

The conceptual model presented in Paragraph 8.4 is used to develop the numerical model. This conceptual model is based on the data which is summarized in Chapter 6. The location of the major upflow zone(s), represented as fault zones in the numerical model, is determined following the location of the surface manifestations and the temperature and chemical composition of the geothermal fluids. Therefore Kawah Putih is thought to correspond with the main upflow zone. As illustrated in the conceptual model presented in Paragraph 8.4, the surface manifestations at Kawah Cibuni and Kawah Ciwidey are the result of upflow of heat from a minor heat source and lateral flow through the reservoir rock from the main upflow zone beneath Kawah Putih.

As discussed in Chapter 6, the cap rock is characterized by the presence of argillic clay minerals, which are formed by the interaction of the geothermal waters with the volcanic rock. The steam cap is formed below the cap rock. The presence of steam is derived from pressure and temperature indications that are obtained from alteration minerals that are identified in the well cores. The occurrence of for example epidote suggests temperatures around 240°C. Since the presence of other minerals suggests that the temperatures can exceed this 240°C, it is suggested that there is a deep liquid-dominated reservoir below the steam cap.

Opposed to the earlier complex model developed by West JEC, a simple and straightforward approach has been proposed by the author. The results show that the Patuha vapor-dominated system can be well represented by a homogeneous reservoir with a few fault zones that initiate fluid flow through the sealing cap rock layer. Although the modeled pressures and temperatures based on the theoretical design of a vapor-dominated reservoir deviate from the well measurement, the obtained profiles resemble the pattern from the field data.

Additional research can be done by further calibrating the presented numerical model of the Patuha vapor-dominated reservoir with the field data. This should result in an accurate natural state model which can be used to estimate the size of the resource in the area. This natural state model can be used to design a sustainable field development plan for the production of steam from the Patuha reservoir.

Acknowledgements

I would like to thank IF Technology and Geo Dipa Energi for giving me the opportunity to do this project, especially my supervisors, Nick Buik and Mariene Guiterrez-Neri (IF Technology) and Puji Sirait, Ruly Husnie Ridwan and M. Istiawan Nurpratama (Geo Dipa Energi) for their help and support. I would also like to thank my thesis supervisor, Prof dr Ruud J. Schotting, for checking my work and providing me with important comments. Furthermore, I would like to thank Rockware, Inc. for providing me with the necessary software to develop the numerical model.

References

Acuna, J.A., J. Stimac, L. Sirad-Azwar, and R.G. Pasikki. (2008). Reservoir management at Awibengkok geothermal field, West Java, Indonesia. *Geothermics* **37**, 332-346.

Allis, R. (2000). Insight on the formation of vapor-dominated geothermal systems. *Proceedings,* World Geothermal Congress 2000, Kyusho-Tohoku, Japan.

Battaglia, M., and P. Segall. (2004). The interpretation of gravity changes and crustal deformation in active volcanic areas. *Pure appl. geophys.* **161**, 1453-1467.

Bertani, R. (2010). Geothermal power generation in the world 2005-2010 update report. *Proceedings,* World Geothermal Congress 2010, Bali, Indonesia.

Bignall, G. (2010). Module 8: Petrology – Hydrothermal alteration. *Internal presentation: Wairakei Research Centre GNS Science.*

Browne, P.R.L. (1978). Hydrothermal alteration in active geothermal fields. *Ann. Rev. Earth Planet. Sci.* **6**, 229-250

Browne, P.R.L., and A.J. Allis. (1970). The Ohaki-Broadlands hydrothermal area, New-Zealand: Mineralogy and related geochemistry. *American Journal of Science* **269**, 97-131.

Darma, S., S. Harsoprayitno, H. D. Ibrahim, A. Effendi , and A. Triboesono. (2010). Geothermal in Indonesia: government regulations and power utilities, opportunities and challenges of its development. *Proceedings,* World Geothermal Congress 2010, Bali, Indonesia.

Dwipa, S., and B. Setiawan. (2005). The Current State of Geothermal Development in Indonesia. *Proceedings,* 42nd CCOP Annual Session 2005, Beijing, China.

Fauzi, A., S. Bahri, and H. Akuanbatin. (2000). Geothermal development in Indonesia: An overview of industry status and future growth. *Proceedings,* World Geothermal Congress 2000, Kyusho-Tohoku, Japan.

Geosystem SRL. (1995). Interpretational report: Geophysics in the Patuha area Jawa Barat, Republic of Indonesia. *Internal report: Patuha Power Ltd.*

GeothermEx, Inc. (1997). Preliminary resource assessment of the Patuha unit 1 project at Patuha geothermal field, Indonesia. *Internal report: Credit Suisse First Boston.*

Hall, R. (2002). Cenozoic geological and plate tectonic evolution of SE Asia and the SW Pacific: Computer-based reconstructions, model and animations. *Journal of Asian Earth Sciences* **20**, 353-431.

Hamilton, W. (1979). *Tectonics of the Indonesian region*. Washington D.C.: United States Government Printing Office.

Ingebritsen, S.E., and M.L. Sorey. (1988). Vapor-dominated zones within hydrothermal systems: Evolution and natural state. *Journal of Geophysical Research* **93**, 13635-13655.

Layman, E.B., and S. Soemarinda. (2003). The Patuha vapor-dominated resource West-Java, Indonesia. *Proceedings,* 28th Workshop on Geothermal Reservoir Engineering 2003, Stanford, California.

Muffler, P.L.J., and D.E. White. (1969). Active metamorphism of Upper Cenozoic sediments in the Salton Sea geothermal field and the Salton Through, Southeatern California. *Geological society of America* Bulletin 80, 157-182.

Mahon, W.A.J., L.E. Klyen, and M. Rhode. (1980). Neutral sodium/bicarbonate/sulphate hot waters in geothermal systems. *Chinetsu (Journal Japan Geothermal Energy Association)* **17,** 11–24.

Nemčok, M., J. Moore, C. Christensen, R. Allis, T. Powell, B. Murray, and G. Nash. (2007). Controls on the Karaha–Telaga Bodas geothermal reservoir, Indonesia. *Geothermics* **36**, 9-46.

Nicholson, K. (1993). *Geothermal fluids: Chemistry and exploration techniques*. Germany: Springer-Verlag

Norman, D.K., W.T. Parry, and J.R. Bowman. (1991). Petrology and geochemistry of propylitic alteration at Southwest Tintic, Utah. *Economic geology* **86**, 13-28.

Setijadji, L.D. (2010). Segmented Volcanic Arc and its Association with Geothermal Fields in Java Island, Indonesia. *Proceedings,* World Geothermal Congress 2010, Bali, Indonesia.

Sigurdsson, H. (1999). *Encyclopedia of volcanoes*. San Diego: Acadamic Press.

Sriwana, T., M.J. van Bergen, and S. Darma. (2001). Penyebaran unsur kimia dari daerah kenampakan panasbumi dan lumpur belerang di Gunung Patuha, Ciwidey, Jawa Barat. *Proceedings,* 5th Inaga Annual Scientific Conference & Exhibitions 2001, Yogyakarta, Indonesia.

Steiner, A. (1968). Clay minerals in hydrothermally altered rocks at Wairakei, New Zealand. *Clays and clay minerals* **16**, 193-213.

Pruess, K., C. Oldenburg, and G. Moridis. (2011) TOUGH2 User's guide, version 2. *Earth Science Division, Lawrence Berkeley National Laboratory*. LBNL-43134 (revised)

USGS and NASA. (2000). DEM data provided by the Shuttle Radar Topography Mission (SRTM). Retrieved from: http://gdex.cr.usgs.gov/gdex/, consulted at 03-13-2013

West Japan Engineering Consultants (West JEC), Inc. (2007). Feasibility study for Patuha geothermal power development: Final feasibility report. *Internal report: Japan Bank International Cooperation (JBIC).*

White, D.E., L.J.P. Muffler, and A.H. Truesdell. (1971). Vapor-dominated hydrothermal systems compared with hot-water systems. *Economic geology* **66**, 75-97.

Appendix A Cross sections of the Patuha geothermal system

The locations of the cross sections are given in Figure 18